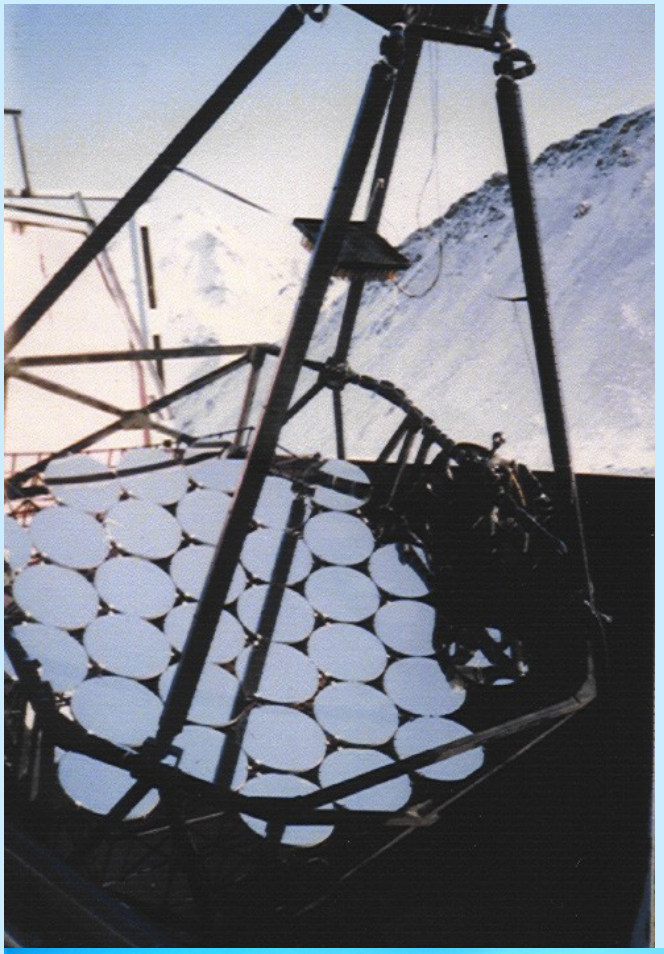

Very high energy gamma-ray emission of Perseus Cluster and NGC 1275

V.G. SINITSYNA, V.Y. SINITSYNA

P. N. Lebedev Physical Institute,
Leninsky prospect 53, Moscow, 119991 Russia

VERY-HIGH ENERGY GAMMA-RAY ASTRONOMY of GALACTIC and EXTRA-GALACTIC SOURCES by SHALON

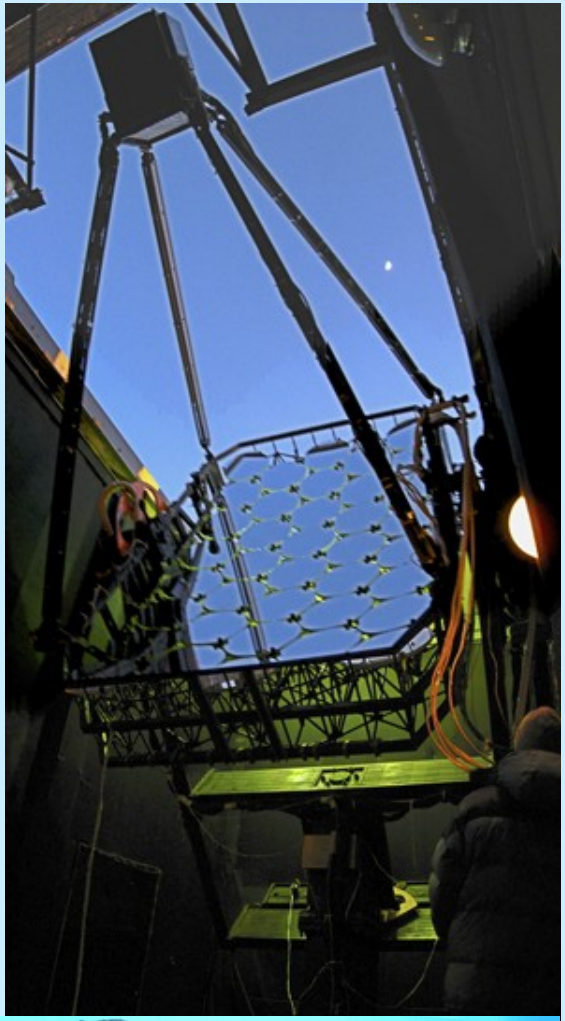

The SHALON Cherenkov gamma-telescope located at 3340 m a.s.l., at the Tien Shan high-mountain observatory of Lebedev Physical Institute, has been developed for gamma - astronomical observation in the energy range 0,8-100 TeV. The gamma – astronomical researches are carrying out with SHALON since 1992. During the period 1992 - 2014 SHALON has been used for observations of metagalactic sources: Mkn 421, Mkn 501, Mkn 180, NGC 1275, SN2006gy, 3c382, OJ 287, 3c454.3, 1739+522 and galactic sources: Crab Nebula, Cyg X-3, Tycho's SNR, Cas A, Geminga, 2129+47XR.

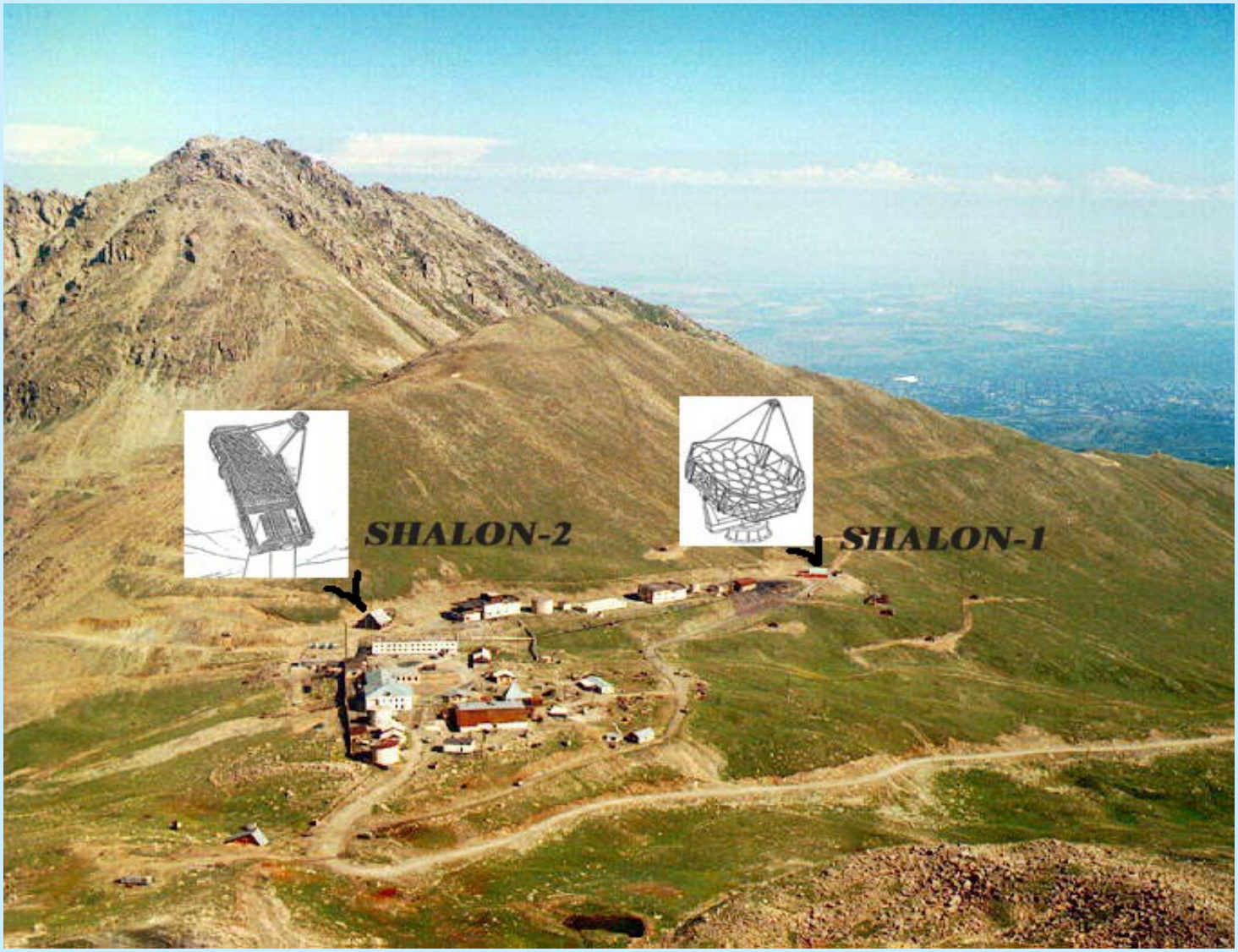
SHALON-2
SHALON-1

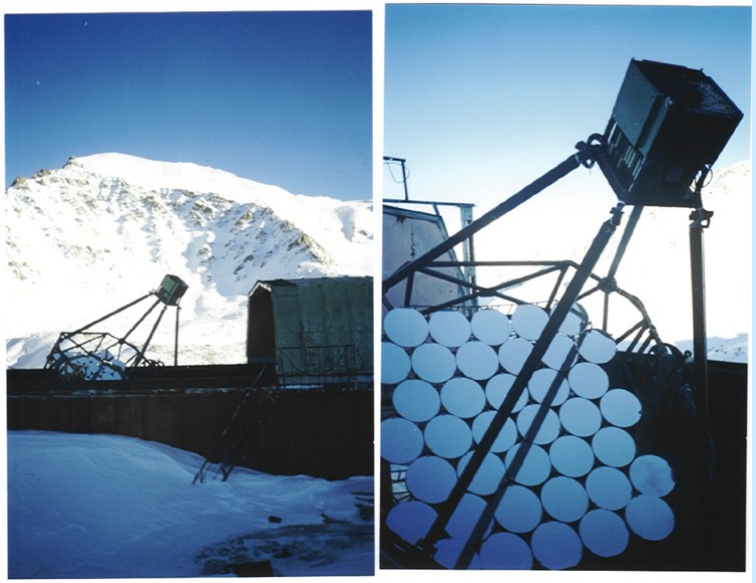

SHALON-1

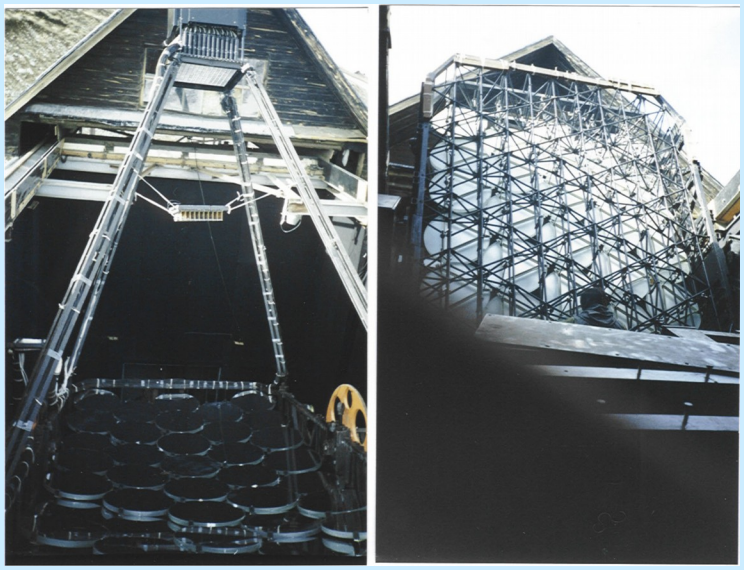

SHALON-2

HIGH MOUNTAINOUS OBSERVATORY SHALON ALATOO

SHALON mirror Cherenkov telescope created at Lebedev Physical Institute and stated in 1991 - 1992

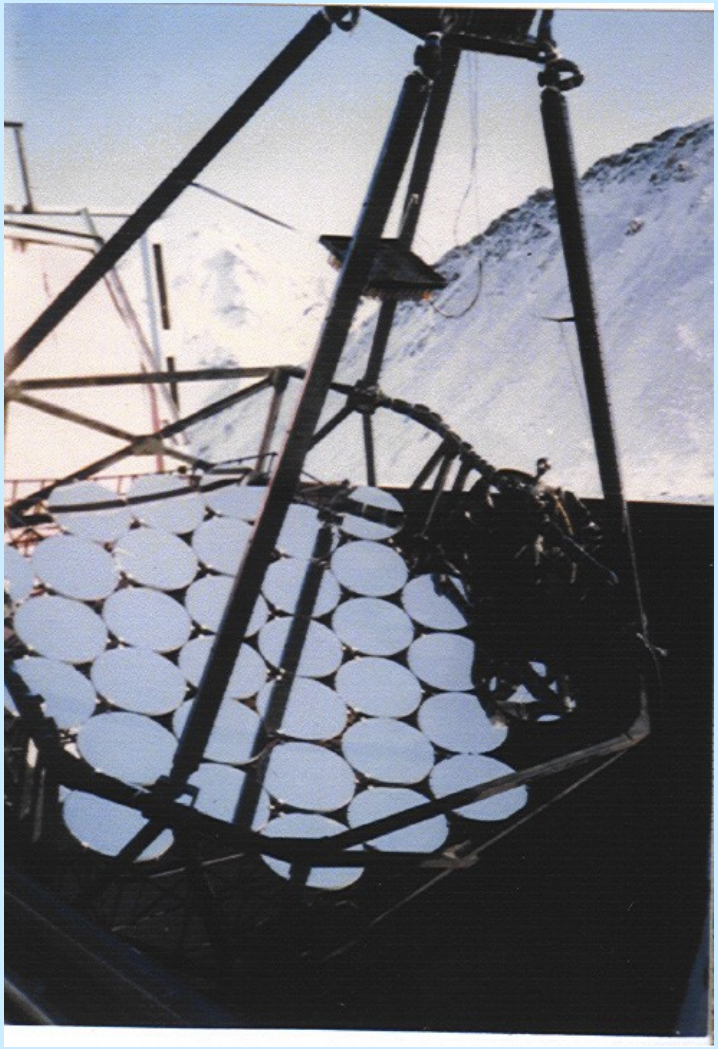

- Total area of spherical mirror — 11.2 m^2
- Radius of mirror curvature — 8.5 m
- The angle range of telescope turn:
  - azimuth — 0°-360°
  - zenith — 0°-110°
- The accurace of telescopic axis pointing — $\leq 0.1^o$
- The photomultiplier tube camera (12x12) — 144 elements
- Field of view > 8°
- Weigth 6 ton
- altazimuth mounting

It is essential that our telescope has a large matrix with full angle >8° that allows us to perform observations of the supposed astronomical source (ON data) and background from extensive air showers (EAS) induced by cosmic ray (OFF data) simultaneously. Thus, the OFF data are collecting for exactly the same atmospheric thickness, transparency and other experimental conditions as the ON data.

Evolution of photomultiplier arrays to record images seen in Cherenkov light

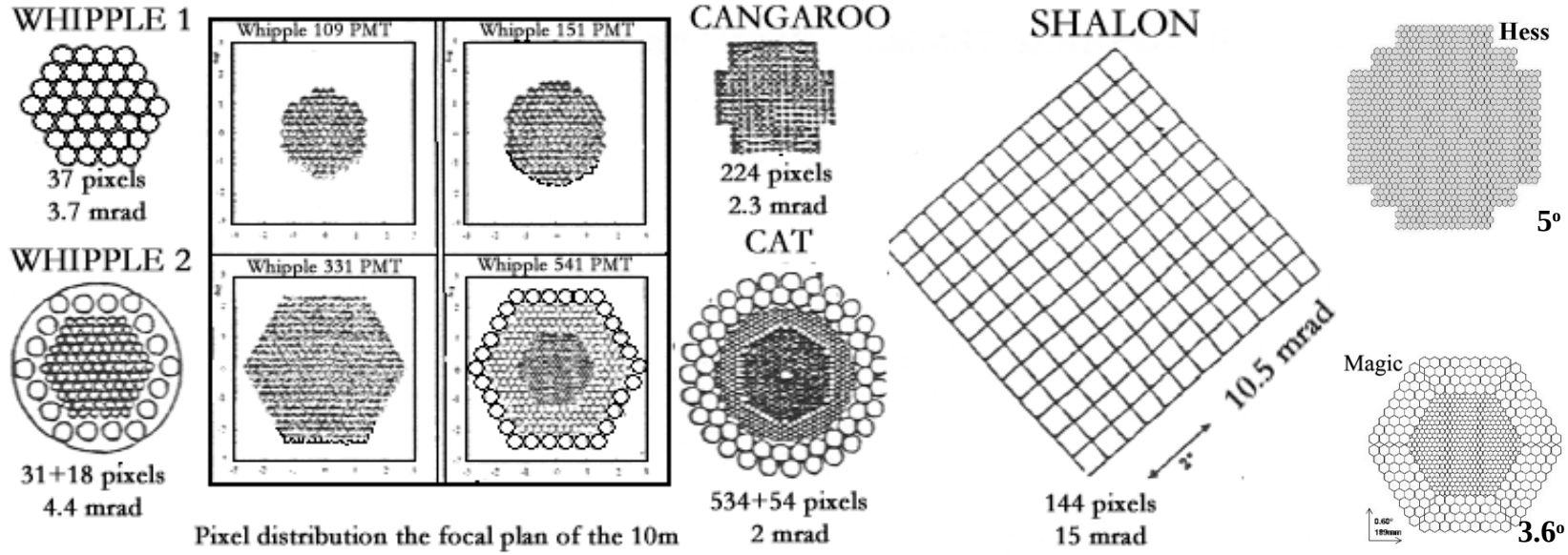

Pixel distribution the focal plan of the 10m reflector: top left: 109 pixels (1993-1996); top right: 151 pixels (Dec.,1996); 331 pixels (Oct., 1997); 541 pixels)

The lightreceiver has the largest field of view in the world, >8°. This allows one to monitor the background from charged cosmic-ray particles and the atmospheric transparency continuously during observations and expands the area of observation and, hence, the efficiency of observations. The technique for simultaneously obtaining information about the cosmic-ray background and the showers initiated by gamma rays is unique and has been applied in the SHALON experiment from the very beginning of its operation. This technique serves to increase the useful source tracking time and, what is particularly important, such source and background observation conditions as the thickness and state of the atmosphere remain the same.

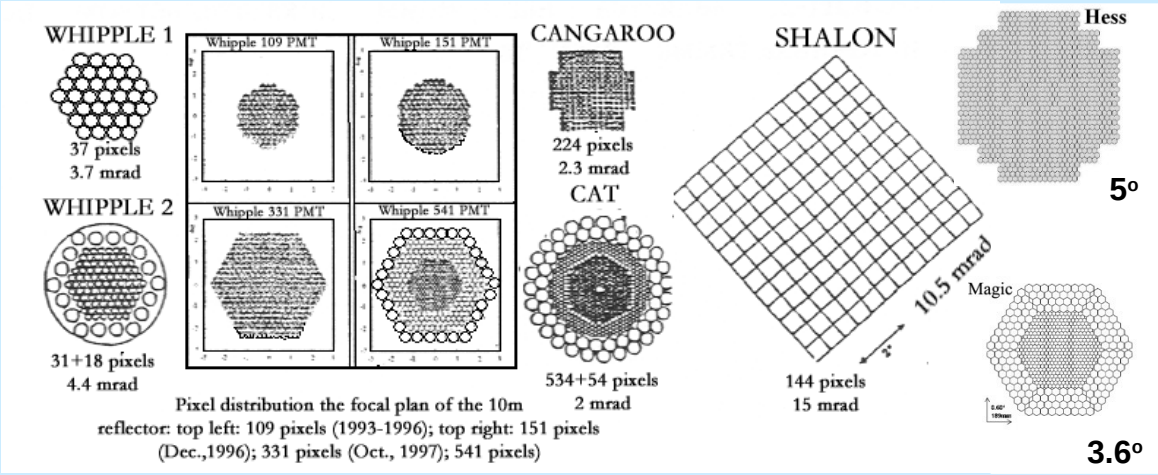

Pixel distribution the focal plan of the 10m reflector: top left: 109 pixels (1993-1996); top right: 151 pixels (Dec.,1996); 331 pixels (Oct., 1997); 541 pixels)

This method is inaccessible to other gamma-ray astronomical experiments, because the telescopes used in the world have a smaller field of view. In addition, the wide field of view allows recording the off-center showers arriving at distances of more than 30 m from the telescope axis completely and almost without any distortions; they account for more 90% of all the showers recorded by the telescope.

During a primary analysis, the primary particle arrival direction is determined with an accuracy up to ≲0.1°. The subsequent analysis specially developed for the SHALON telescopes and based on Tikhonov's regularization method improves the accuracy to a value of less than 0.01°.
[V.G. Sinitsyna, V.Y. Sinitsyna, Astron. Lett. 40(2-3), 75 (2014)]

SHALON sky-map catalogue of γ -quantum sources 800 GeV – 100TeV (2015)

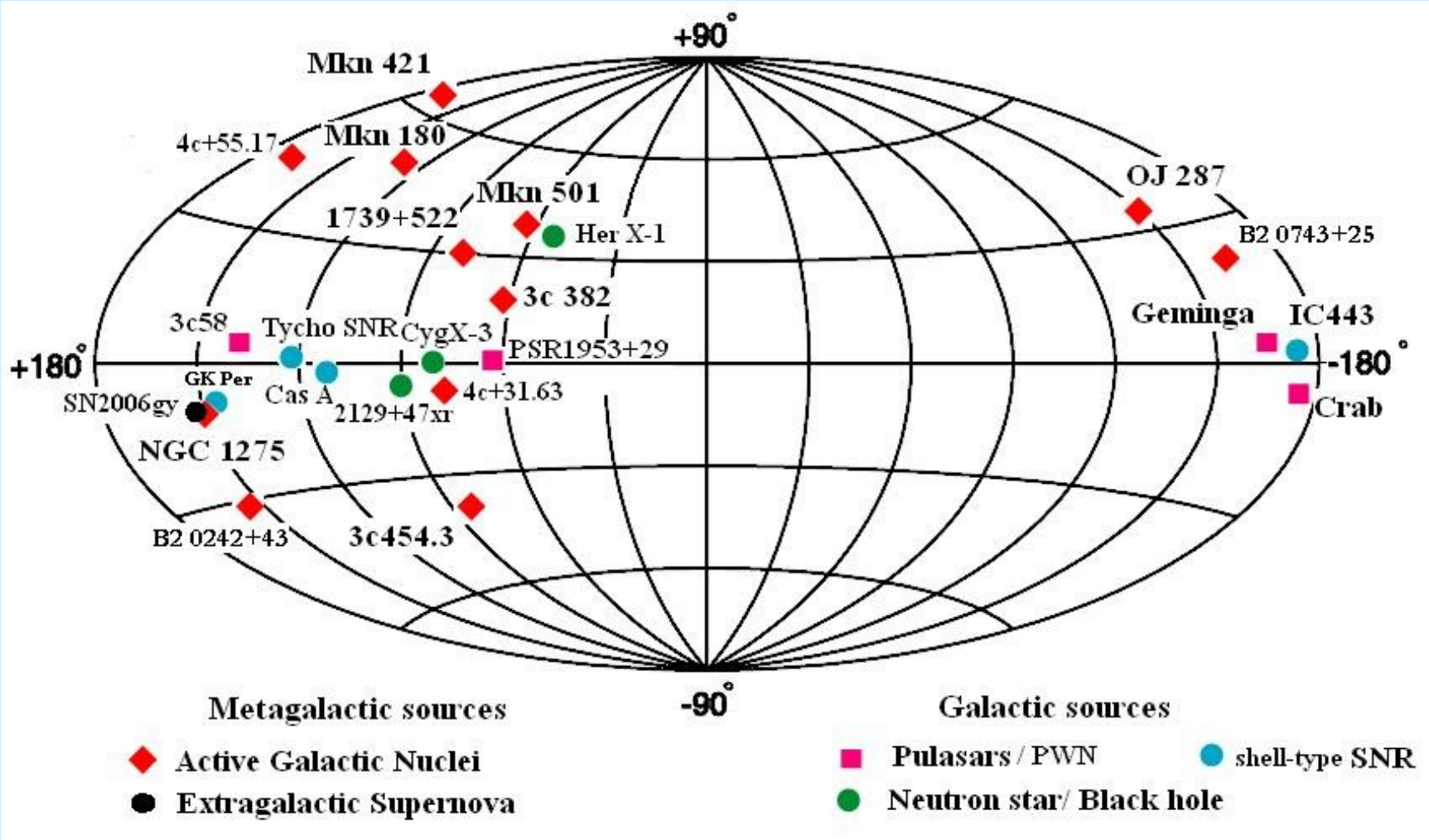

SHALON catalogue of metagalactic γ -quantum sources 800 GeV – 100TeV (2015)

Source	Source type	Observed Flux, $cm^{-2}s^{-1}$	Distance		Detected** by SHALON	Detected at high energies Experiment/year	Detected at very high energies Experiment/year
Galactic			*kpc*				
Crab Nebula	Plerion, PWN	$(2.12\pm0.12)\times10^{-12}$	2.0		1995[1]	COS-B/1987 [15] (FermiLAT/2009)	Whipple/1989 [16]
* Geminga	Radio-weak pulsar/ Plerion (?)	$(0.48\pm0.07)\times10^{-12}$	0.25		2000[5]	COS-B/1981 [18] EGRET/1994 [19] (FermiLAT/2009)	Crimea/2001 [49] MILAGRO/2007 [20]
* 3c 58	Plerion, PWN	$(0.56\pm0.15)\times10^{-12}$	2.6 - 3.2		2012[14]	FermiLAT/2009 [27]	*(VERITAS/2006 UL)*
SNR 1181 (?)	Plerion, PWN (?)	$(1.40\pm0.43)\times10^{-12}$	2.6 - 3.2 (?)		2012[14]	FermiLAT/2009 [27]	–
* GK Per(Nova1901)	Classical Nova	$(0.31\pm0.14)\times10^{-12}$	0.46		2015[54]	–	–
* Tycho's SNR	Shell-type SNR	$(0.52\pm0.04)\times10^{-12}$	2.5 – 3,5		1998[4]	FermiLAT/2011 [24]	VERITAS/2011 [23]
Cas A	Shell-type SNR	$(0.64\pm0.10)\times10^{-12}$	3,1		2011[12]	FermiLAT/2010 [26]	HEGRA/2001 [25]
IC 443	Shell-type SNR	$(1.69\pm0.58)\times10^{-12}$	1.5		2012[14]	EGRET/1996 [21] (FermiLAT/2009)	MAGIC/2007 [22]
* γCygni SNR	Shell-type SNR	$(1.27\pm0.11)\times10^{-12}$	1.5		2013 [50]	EGRET/1996 [21] (FermiLAT/2009)	VERITAS/2013 [51]
* Cygnus X-3	Binary	$(0.68\pm0.04)\times10^{-12}$	10		1997[2]	EGRET/1997[29] (FermiLAT/2009[30])	Crimea/2009 [48] (*Crimea/1975* [28])
* 2129+47XR	Low-mass X-ray Binary	$(0.19\pm0.06)\times10^{-12}$	6.0		2006[7]	–	–
* Her X-1	Binary	$(0.45\pm0.18)\times10^{-12}$	6.6		2012	–	*(Whipple UL)*
* M57	Planetary nebula	$(0.30\pm0.17)\times10^{-12}$	0.7		2011[13]	–	–
Extragalactic			*Mpc*	*z*			
* NGC 1275	Seyfert Galaxy	$(0.78\pm0.05)\times10^{-12}$	71	0.0179	1997[3]	FermiLAT/2009 [31]	MAGIC/2012 [32]
* SN2006 gy	Extragal.Supernova	$(3.71\pm0.65)\times10^{-12}$	73	0.019	2007[9]	–	–
Mkn 421	BLLac	$(0.63\pm0.05)\times10^{-12}$	124	0.031	1995[1]	EGRET/1992 [35](FermiLAT/2009)	Whipple/1992 [33]
Mkn 501	BLLac	$(0.86\pm0.06)\times10^{-12}$	135	0.034	1997[1a]	EGRET/1999 [37](FermiLAT/2009)	Whipple/1996 [34]
Mkn 180	BLLac	$(0.65\pm0.09)\times10^{-12}$	173	0.046	2009[10]	FermiLAT/2009 [39]	MAGIC/2006 [38]
* 3c382	Broad Line Radio Galaxy	$(0.95\pm0.33)\times10^{-12}$	230	0.058	2010[11]	*(FermiLAT UL)* [40]	–
* 4c+31.63	FSRQ	$(0.72\pm0.22)\times10^{-12}$	1509	0.295	2013	FermiLAT/2010 [47]	–
* OJ 287	BLLac	$(0.26\pm0.07)\times10^{-12}$	1576	0.306	*2005* [8]*(UL)* 2010[11]	FermiLAT/2009 [41]	*(MAGIC / 2009 UL)* [42]
* 3c454.3	FSRQ	$(0.43\pm0.07)\times10^{-12}$	5489	0.859	2000[6]	FermiLAT/2009 [44]	*(MAGIC / 2009 UL)* [45]
* 4c+55.17	FSRQ	$(0.91\pm0.25)\times10^{-12}$	5785	0.896	2013	FermiLAT/2011 [43]	–
* 1739+522 (4c+51.37)	FSRQ	$(0.49\pm0.05)\times10^{-12}$	9913	1.375	2000[6]	FermiLAT/2010 [46]	–
* B2 0242+43	FSRQ	$(0.58\pm0.20)\times10^{-12}$	16865	2.243	2015	FermiLAT/2010, 2011	–
* B2 0743+25	FSRQ	$(0.37\pm0.16)\times10^{-12}$	23466	2.949	2015	FermiLAT/2010, 2011	–

TeV GAMMA-RAY EMISSION from METAGALACTIC SOURCES

The gamma-astronomical researches are carrying out with SHALON mirror telescope at the Tien-Shan high-mountain observatory. During the period 1992 - 2015, SHALON has been used for observations of the metagalactic sources Mkn421, Mkn501, NGC1275, OJ 287, 3c454.3, 1739+522 and galactic sources Crab Nebula, Cygnus X-3, Tycho's SNR, Geminga, 2129+47XR.

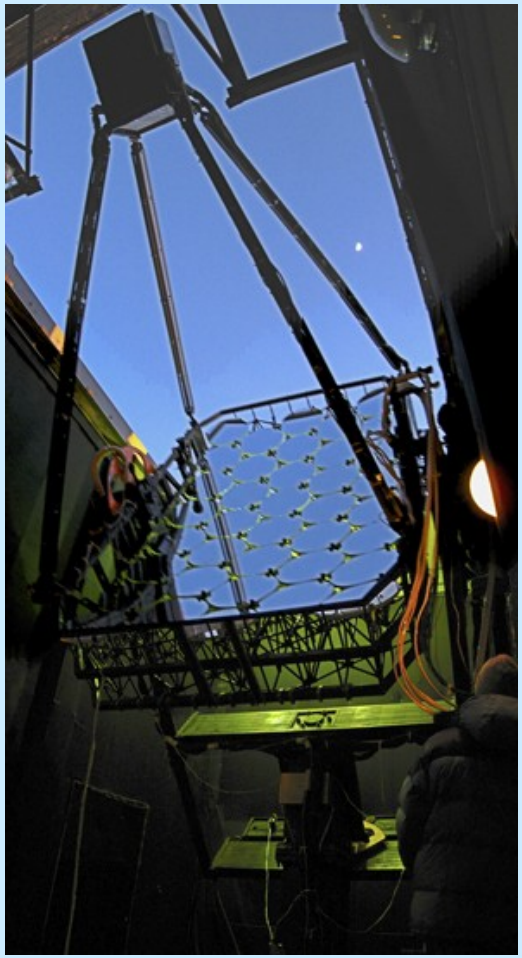

SHALON catalogue of metagalactic γ -quantum sources

Source	Observable flux, $cm^{-2}s^{-1}$	z	Source type
NGC 1275	$(0.78\pm0.05)\times10^{-12}$	0.0179	Syefer Galaxy
SN2006 gy	$(3.71\pm0.65)\times10^{-12}$	0.019	Extragalactic Supernova
Mkn 421	$(0.63\pm0.05)\times10^{-12}$	0.031	BLLac
Mkn 501	$(0.86\pm0.06)\times10^{-12}$	0.034	BLLac
Mkn 180	$(0.65\pm0.09)\times10^{-12}$	0.046	BLLac
3c382	$(0.95\pm0.20)\times10^{-12}$	0.0579	Radio Galaxy
4c+31.63	$(0.72\pm0.22)\times10^{-12}$	0.295	FSRQ
OJ 287	$(0.26\pm0.07)\times10^{-12}$	0.306	BLLac
3c4543	$(0.43\pm0.07)\times10^{-12}$	0.859	FSRQ
4c+55.17	$(0.93\pm0.28)\times10^{-12}$	0.896	FSRQ
1739+522	$(0.49\pm0.05)\times10^{-12}$	1.375	FSRQ
B2 0242+43	$(0.58\pm0.20)\times10^{-12}$	2.243	FSRQ
B2 0743+25	$(0.37\pm0.16)\times10^{-12}$	2.949	FSRQ

Active Galactic Nuclei

The dominant galaxy in the Perseus cluster is NGC 1275.

The SHALON observations of Seyfert galaxy NGC 1275 are presented. The observation results can help both to solve the problem of origin and acceleration of very high energy γ-rays thus the dynamics of outflows in the active galaxy and clarify the difference between the different classes of AGNi .

In the last years, high and very high energy γ-rays have come to play an important role in the study of Active Galactic Nuclei. A big number of AGNi have been detected through the MeV to TeV energies. Also, active galaxies are intensely studied in all wavelengths.

The cluster of galaxies in Perseus is one of the best-studied clusters due to its relative proximity (its distance $\sim$100 Mpc or redshift z = 0.0179) and brightness. Clusters of galaxies have long been considered as possible candidates for the sources of TeV gamma rays emitted by protons and electrons accelerated at large-scale shocks or by a galactic wind or active galactic nuclei (Dennison 1980; Houston et al. 1984; Colafrancesco and Blasi 1998; Sarazin 1999; Miniati et al. 2001; Timokhin et al. 2004; Colafrancesco and Marchegiani 2009).

NGC 1275

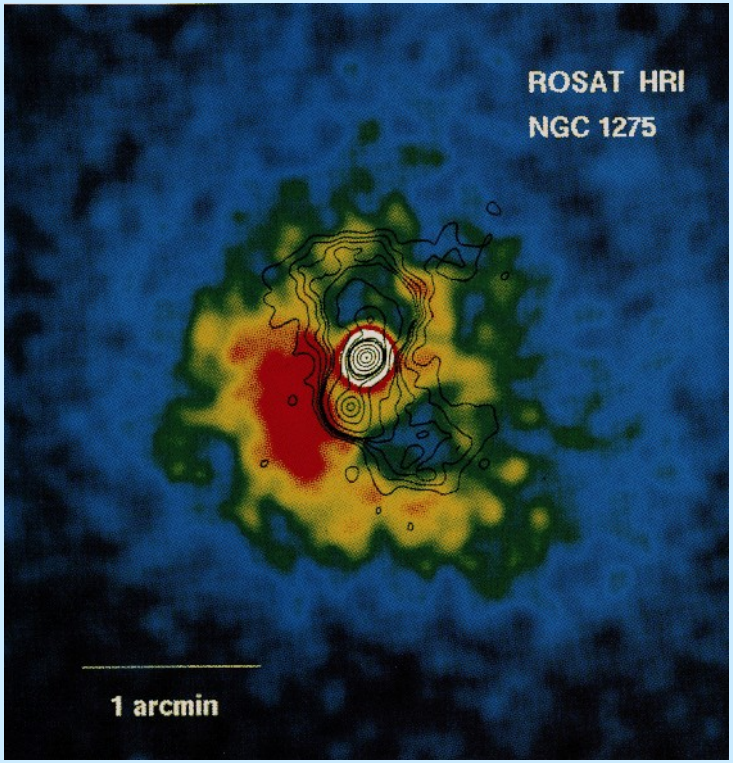

A ROSAT HRI image of the region around the galaxy NGC 1275 at the centre of the Perseus galaxy cluster. The contour lines show the radio structure as given by VLA observations. The maxima of the X-ray and radio emission coincide with the active nucleus of NGC 1275. In contrast, the X-ray emission disappears almost completely in the vicinity of the radio lobes.

NGC 1275 is a powerful source of radio and X-ray emission. In the radio band, the object found in NGC 1275, also known as 3C 84, has a powerful and compact core that has been well studied with VLBI. NGC 1275 is extremely bright in the radio band; its structure consists of a compact central source and an extended jet. The radio emission extends to large distances and shows a clear interaction with the gas inside the Perseus cluster of galaxies. ROSAT and, then, Chandra observations revealed cavities in the gas located inside the cluster, whose presence suggests that the jets from NGC 1275 sweep up numerous “bubbles” in the atmosphere of the Perseus cluster.

The galaxy NGC 1275 historically aroused great interest due to both its position at the center of the Perseus cluster and its possible “feedback” role (Gallagher 2009). Evidence for the “feedback” role of NGC 1275 can be obtained from ROSAT and Chandra observations, which reveal shells of hot gas and cavities that spatially coincide with the radio structures extending from the central, active part of the AGN.

NGC 1275

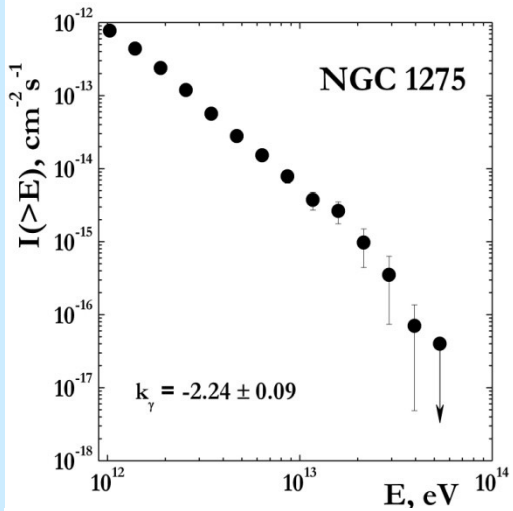

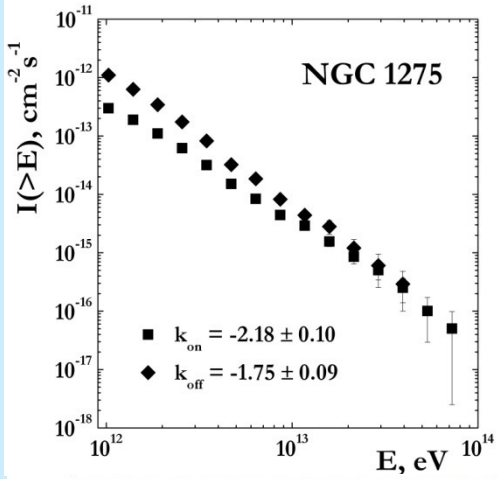

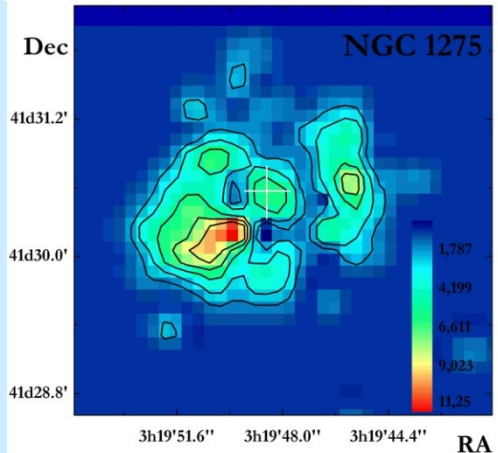

In 1996 year a new metagalactic source are detected by SHALON in TeV energies. This object was identified with Seyfert galaxy NGC 1275.

NGC 1275 was observed by the SHANON telescope for 271.2 h in different years (from 1996 to 2012) during the clear moonless nights at zenith angles from 3° to 33°. The observations were performed using the standard (for SHALON) technique of obtaining information about the cosmic-ray background and gamma-ray-initiated showers in the same observing session. Gamma-ray emission from NGC 1275 was detected by the SHALON telescope at energies above 800 GeV at the 31.4σ confidence level determined according to Li and Ma (1983).

The integral γ-ray flux for this source is found to be $(0.78\pm0.05)\times10^{-12}$ cm^{-2}s^{-1} at energies of > 0.8 TeV. The energy spectrum of NGC 1275 at >0.8 TeV can be approximated by the power law $F(>E_O)\propto E^{k\gamma}$, with $k_\gamma = -2.24 \pm 0.09$.

The spectra of events satisfying the selection criteria (spectral index k_{ON}=-2.18±0.10) and of the background events observed simultaneously with the source (spectral index k_{OFF}=-1.75±0.09) are both shown in comparison.

NGC 1275

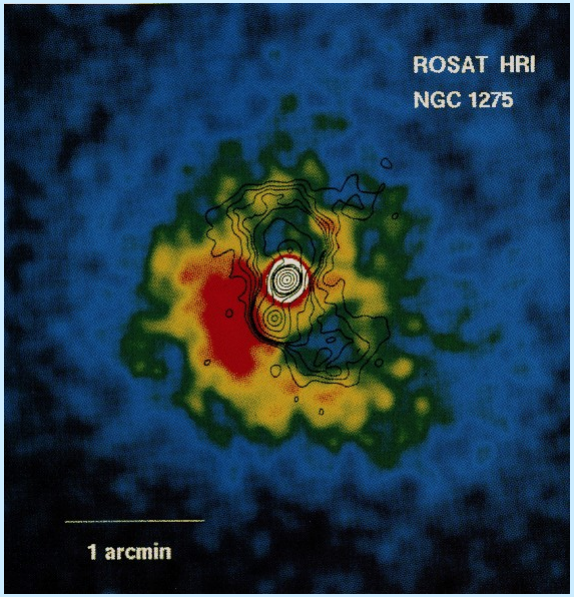

Possible correlations between the emission regions of TeV gamma rays and low-energy (radio and X-ray) photons should be established to found the mechanisms of the generation of very high energy emission.

We also combined the SHALON (0.8–40 TeV) and Chandra (1.5–3.5 keV X-ray) images. In the X-ray energy range, the core of the Perseus cluster, on the whole, appears as a clear circularly symmetric structure with a maximum on NGC 1275.

The clearly seen decreasing in Chandra X-ray flux correlates with the components of the extended double radio structure 3C 84. These areas are surrounded by bright (at energies 1.5–3.5 keV) arc regions from the north and the south. The simplest interpretation is that the intense emission from these arcs comes from the shells surrounding the radio lobes. A bright emission spot is also observed to the east.

The emission regions of very high energy gamma rays observed by SHALON from NGC 1275 well correlates with the photon emission regions in the energy range 1.5–3.5 keV.

Thus, the TeV gamma-ray emission recorded by SHALON from NGC 1275 has an extended structure with at core centered at the source's position.

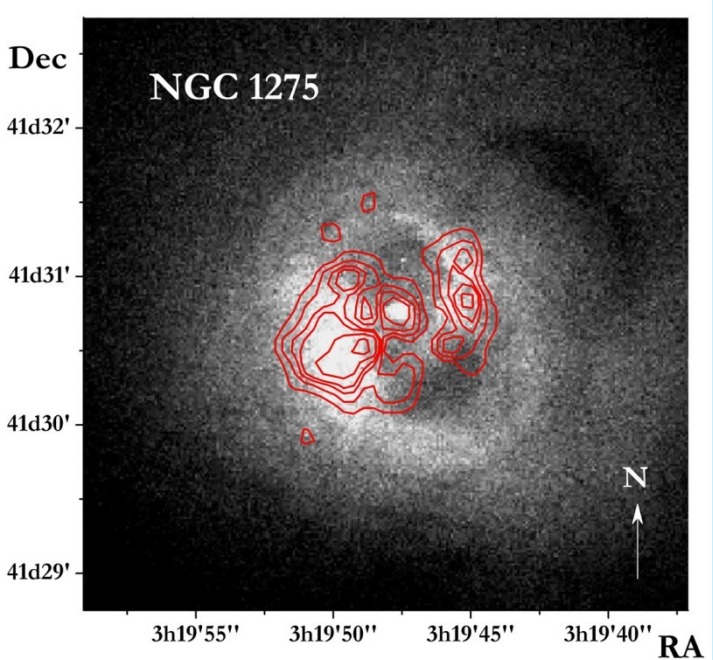

NGC 1275 image: (black-and-white scale) presents a Chandra X-ray (1.5–3.5 keV) image for the central part of the Perseus cluster centered on NGC 1275 with a size of ∼5.5 arcmin.

The contour lines show the 0.8 – 40 TeV - structure by SHALON observations.

NGC 1275

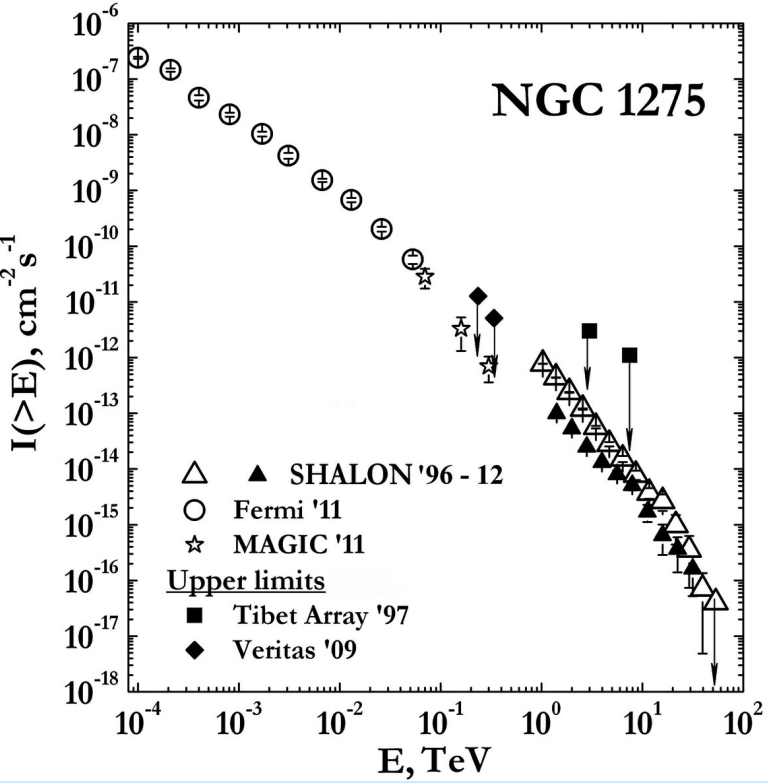

To analyze the emission related to this core, we additionally identified the emission component corresponding to the central region of NGC 1275 with a size of 32”. The emission from the central region of NGC 1275 was detected at energies above 0.8 TeV at a 13.5σ confidence level determined by the Li&Ma method with a average integral flux:

$$I(>800\ \text{GeV}) = (3.26\pm0.3)\times10^{-13}\ \text{cm}^{-2}\text{s}^{-1}.$$

The gamma-ray energy spectrum of the central component in the entire energy range from 0.8 to 40 TeV is well described by a power law with an exponential cutoff,

$$I(>E_\gamma)=(2.92\pm0.11)\times10^{-13}\times E_\gamma^{-1.55\pm0.10}\times\exp(-E_\gamma/10\text{TeV})\text{cm}^{-2}\text{s}^{-1}$$

The integral gamma-ray spectrum of NGC1275 and its central region obtained from SHALON data (1996–2012) with the Fermi LAT (2009–2011) and MAGIC (2010–2011) experimental data.

The SHALON spectrum corresponding to the emission from the central region of NGC 1275 is represented by the black triangles

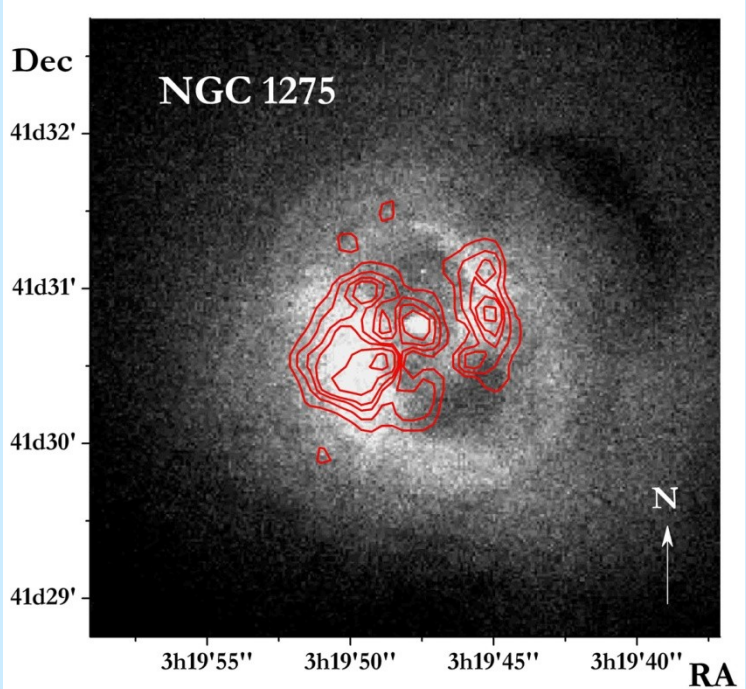

NGC 1275

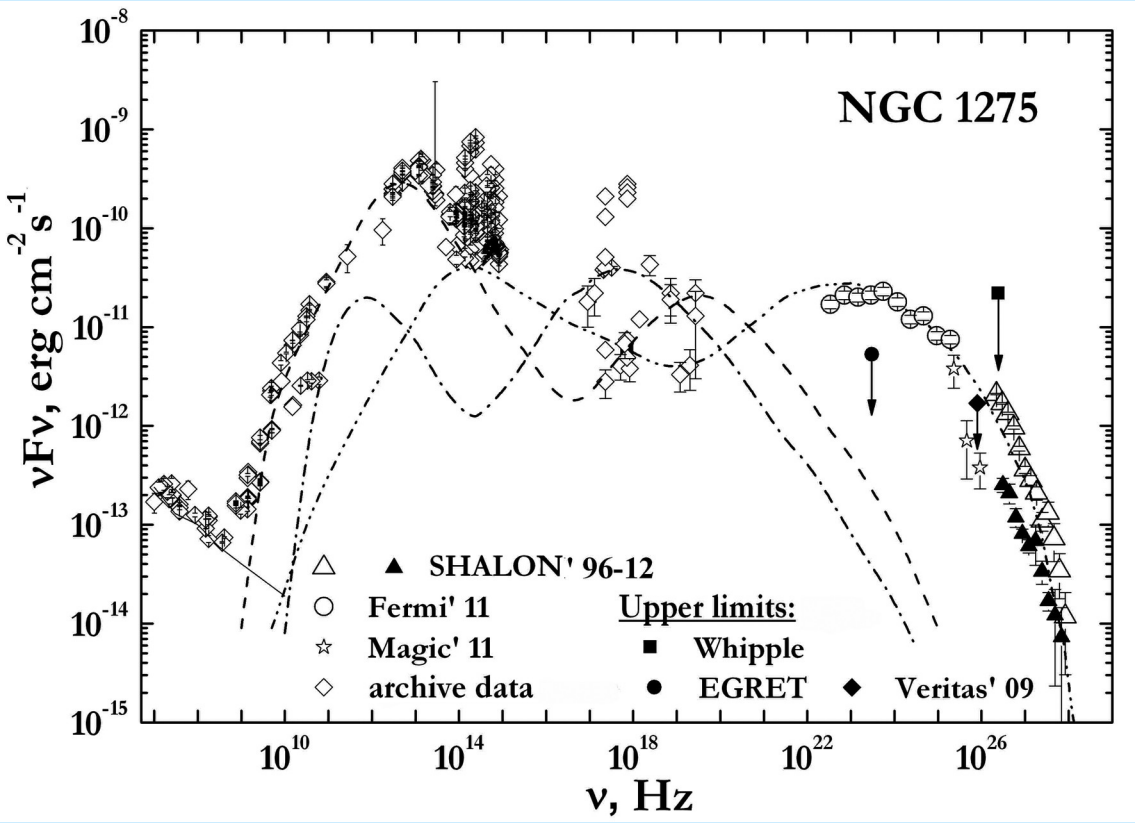

Upper limits on the gamma-ray emission from the Perseus cluster of galaxies and its central galaxy NGC 1275 were obtained in various satellite experiments. The first observations were performed with the COS-B telescope from 1975 to 1979 and then with the EGRET in 1995.

At very high energies, upper limits were obtained in different years in ground-based experiments, such as the large-area scintillation

Tibet Array at E> 3 TeV (1999), and at the Cherenkov telescopes

Whipple(2006) at energies >400 GeV,

MAGIC(2009) at E > 100 GeV, and Veritas (2009) at E > 188 GeV.

The overall spectral energy distribution of NGC 1275 from the low energies to the TeV energies is presented and discussed.

Recently, NGC 1275 was recorded at high energies, 100 MeV– 300 GeV, by the Fermi LAT satellite telescope. To understand the emission generation processes in the entire energy range, the spectral energy distribution should be extended up to very high energies.

Variability of the Gamma-ray Emission from NGC 1275

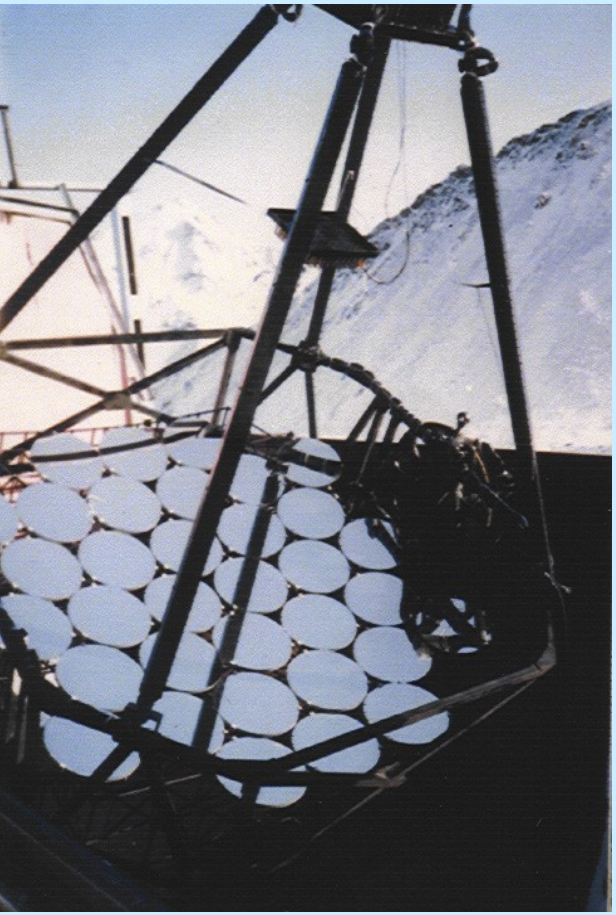

The revealing flares and their duration in long-term observations with mirror Cherenkov telescopes is complicated by the fact that the technique makes a continuous tracking of the source impossible, because it requires such conditions as moonless nights, which already creates a gap in the data for more than ten days; an ideal atmosphere without clouds and, in addition, the source's passage at a distance of no more than 35◦ from zenith are needed, because the influence of a change in atmospheric thickness should be minimal. Nevertheless, revealing correlations between the emissions in different energy ranges, comparing the emission regions, and, in particular, the detection of the flux changes remains necessary, because it makes it possible to judge the nature of the source, its evolution, and the emission generation mechanisms in various objects.

The observed γ-ray flux variations, on average, do not exceed 20% of $(7.8\pm0.5)\times10^{-13}$ cm^{-2} s^{-1}. The SHALON has detected three short-time (within five days) increases and one decrease of the very high energy γ-ray flux. Given these variations, the flux decrease below the average was recorded in 1999 and the integral flux was $(4.7\pm1.3)\times10^{-13}$ cm^{-2} s^{-1}.

Variability of the Gamma-ray Emission from NGC 1275

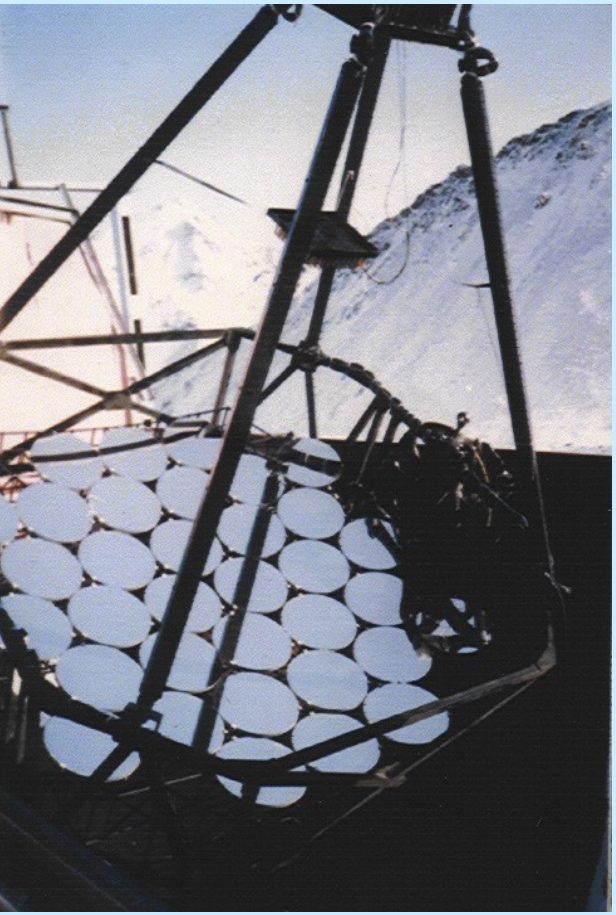

The increases were detected in late January 2001, late November–early December 2005, and late October 2009. The fluxes in these periods were $(21.2\pm7.5)\times10^{-13}$, $(35.5\pm12.4)\times10^{-13}$, and $(23.4\pm4.5)\times10^{-13}$ cm^{-2} s^{-1}, respectively. The duration of the flux increase in October 2009 was 3 days. No intervals of flux increase were found in 2001 and 2005, because the observations were interrupted due to weather conditions in both cases.

To reveal possible correlations of the emissions in various energy ranges, including those at high and very high energies, we compared the NGC 1275 gamma-ray fluxes by SHALON in the periods when the observations were simultaneous with the ones by the Fermi LAT experiment. The published Fermi LAT data were obtained from August 4, 2008, to September 30, 2010 (Brown and Adams 2011). The SHALON observations of NGC 1275 were performed in November 2008 with a break for the Moon's time, October 2009, and mid-November–early December 2010. In this time, only one gamma-ray flux increase to $(23.4 \pm 4.5)\times10^{-13}$ cm^{-2} s^{-1} was detected in the period of October 18–20, 2009. These periods of SHALON observations do not coincide with the times of the main flares observed at Fermi LAT (Brown and Adams 2011). A slight local flux increase can be seen in the period of mid-October 2009 (Brown and Adams 2011), which corresponds to the above-mentioned gamma-ray flux increase observed by SHALON.

SN2006 gy

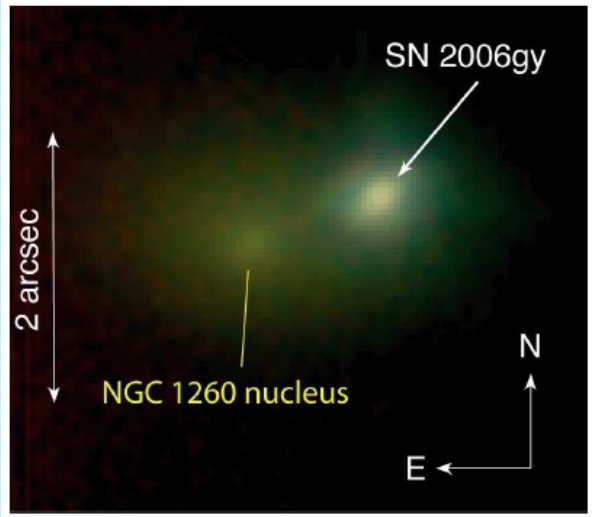

Laser guide star adaptive optics image of SN 2006gy and the nucleus of NGC 1260, showing a clear offset of the SN from the galaxy center. Blue is J band (1.25 μm), green is H band (1.65 μm), and red is Ks band (2.2 μm) on the Shane 3-m telescope at Lick Observatory. [Smith et. all, 2007]

The flux increase was detected from the region NGC 1275 in autumn 2006. The detailed analysis of gamma-shower direction turned out the detection of metagalactic object. This object was identified with the supernova SN 2006gy that is about 10 minutes away from NGC 1275.

Observations had been done in cloudless nights of moonless periods of 2006 Sep., Oct., Nov. Dec. and then during the winter of 2007. No flux increase was found in September observations. In the flare, observed on Oct. 22, the flux increased 6 times from the NGC 1275 and stayed on this level all Oct. moonless period. The integral gamma-ray flux for SN 2006gy is found to be $(3.71\pm0.65)\times10^{-12}$ $cm^{-2}s^{-1}$ at energies of > 0.8 TeV. The energy spectrum of SN2006 gy at 0.8 to 7 TeV can be approximated by the power law $F(>E_O)\propto E^{k\gamma}$, with $k\gamma = -3.13 \pm 0.27$. An images of gamma-ray emission from SN2006 gy by SHALON telescope are presented. Follow-up observations on end of Nov. Showed that the flux of SN2006 gy had dropped to a flux level of about $(0.69\pm0.17)\times10^{-12}$ $cm^{-2}s^{-1}$ and was constant during the Nov. Dec. period. The results of observation analysis of 2007 have no revealed TeV gamma-ray emission from region of SN 2006gy. So, the explosion of extragalactic supernova was observed at TeV energies for the first time with SHALON Cherenkov telescope.

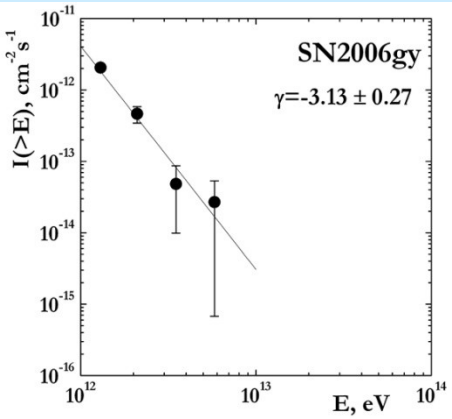

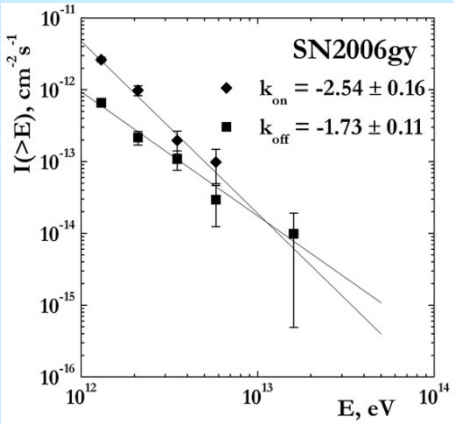

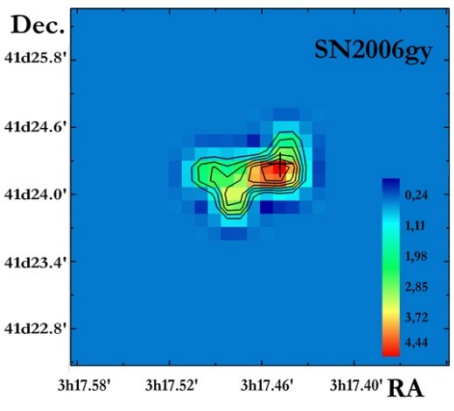

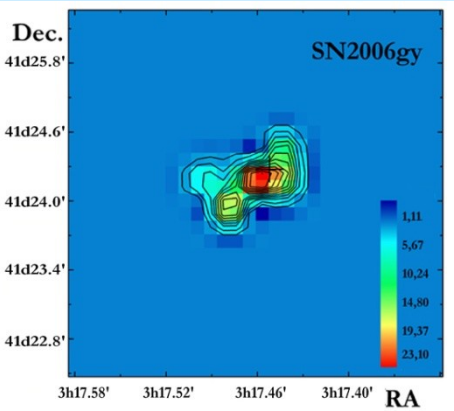

GK Per (Nova 1901)

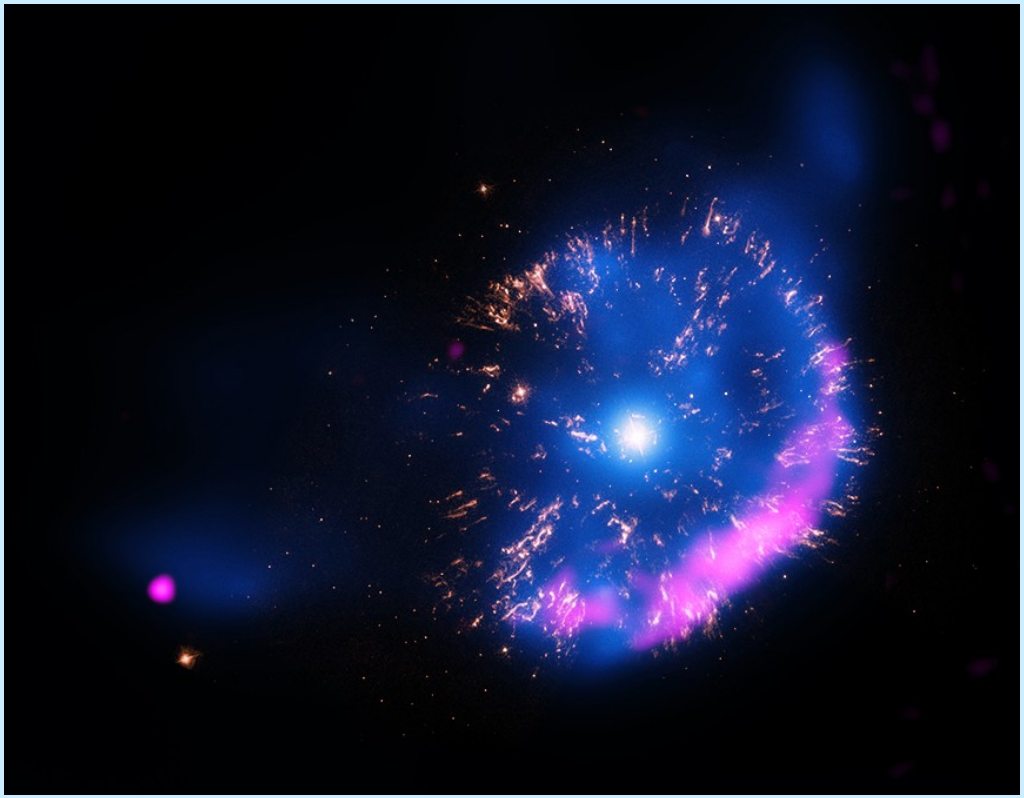

The composite image of GK Per:

- X-rays (blue) from Chandra observations
- optical data (yellow) from NASA's Hubble Space Telescope
- radio data (pink) from the National Science Foundation's Very Large Array

Nova Persei 1901 (GK Per) is one of the most extensively observed and studied classical nova shells over the entire electromagnetic spectrum. The optical data are demonstrated interaction between the nova ejecta and the ambient gas. Furthermore, remnant of nova is detected at radio energies with the Very Large Array (VLA) as a source of nonthermal, polarized radio emission. The results of these observations show the existence of shocked interstellar material. The X-ray shell around GK Per was first discovered with the ROSAT experiment and then it has been observed by Chandra telescope. In particular, with Chandra observations, the X-ray emission of the same electron population has been detected as the extension from the radio wavelengths. The detection of the X-rays from the supernova remnant shell which are primarily due to bremsstrahlung of shock accelerated relativistic electrons, supposed the detection of γ-ray emission originated from π°- decay, secondary pp-interactions as well as possible contribution emission produced via Inverse Compton scattering. Chandra X-ray data shows that, the nova remnant of GK Per could be a younger remnant that will resemble older SNRs like IC 443 $\sim (3\div30)\times10^{3}$ year which interact with molecular clouds.

GK Per (Nova 1901)

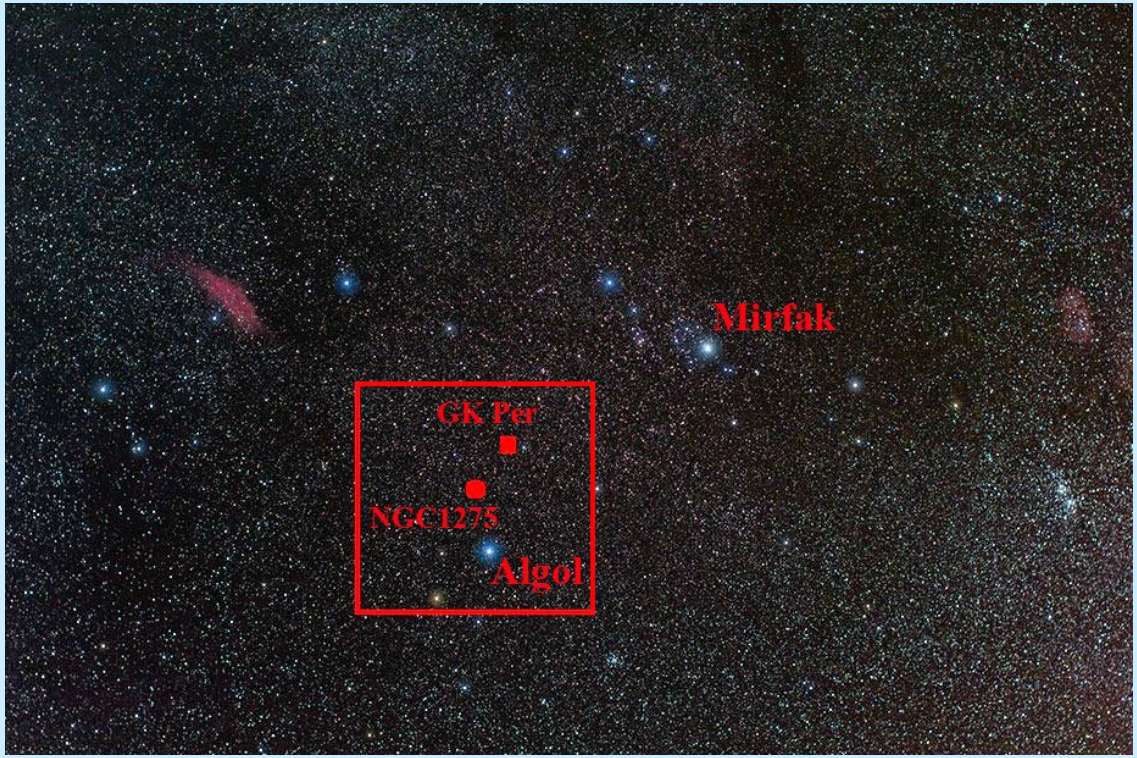

During the observations of NGC1275 the SHALON field of view contains GK Per as it located at ~3° North from NGC1275. So due to the large telescopic field of view (~8°) the observations of NGC1275 is naturally followed by the observations of GK Per.

SHALON telescope field of view during the observation of NGC 1275

GK Per as a source accompanying to NGC 1275 was observed with SHALON telescope at the period 1996y to 2012y for a total of 111 hours. The γ-ray source associated with the GK Per was detected above 2 TeV with a statistical significance 9.2σ determined by Li&Ma and with average gamma-ray flux:

$$\mathbf{I_{GK\ Per}(>2TeV) = (2{,}9\pm13)\bullet10^{-13}\ cm^{-2}s^{-1}}$$

[V.G. Sinitsyna, V.Y. Sinitsyna, 2015, Bull. of the Lebedev Physics Institute, v. 42(6), pp. 169 – 175]

GK Per (Nova 1901)

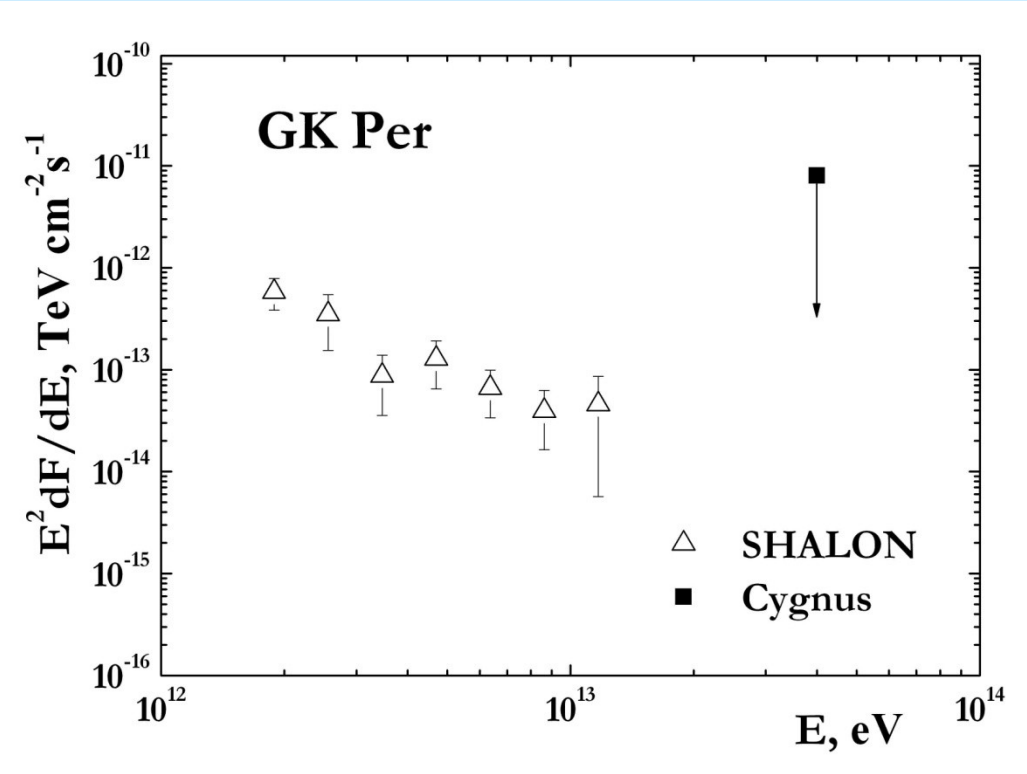

The spectral energy distribution of the *gamma*-ray emission from GK Per by SHALON (Δ) in comparison with other experiment data.

The analysis of γ-ray shower arrival direction revealed the main TeV-emission region coinciding with the position of central source of **classical nova GK Per** and the weak emission of **shell**, that is also observed in X-ray by Chandra (red lines)

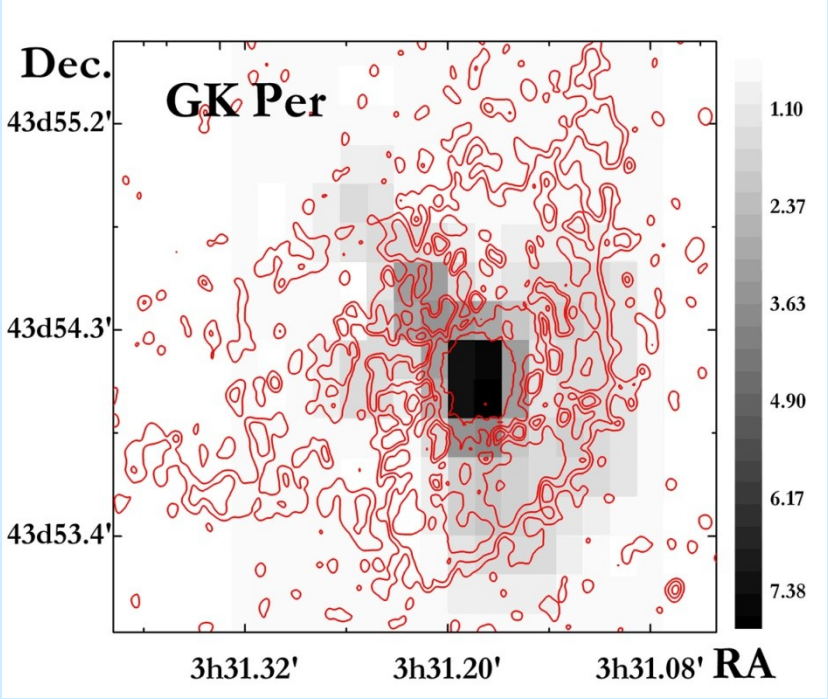

The energy spectrum of γ-rays in the observed energy region from 2 to 15 TeV is well described by the power law: $F(E > 2TeV) \propto E^{k\gamma}$, with $k_\gamma = -1.90 \pm 0.35$

[V.G. Sinitsyna, V.Y. Sinitsyna, 2015, Bull. of the Lebedev Physics Institute, v. 42(6), pp. 169 – 175]

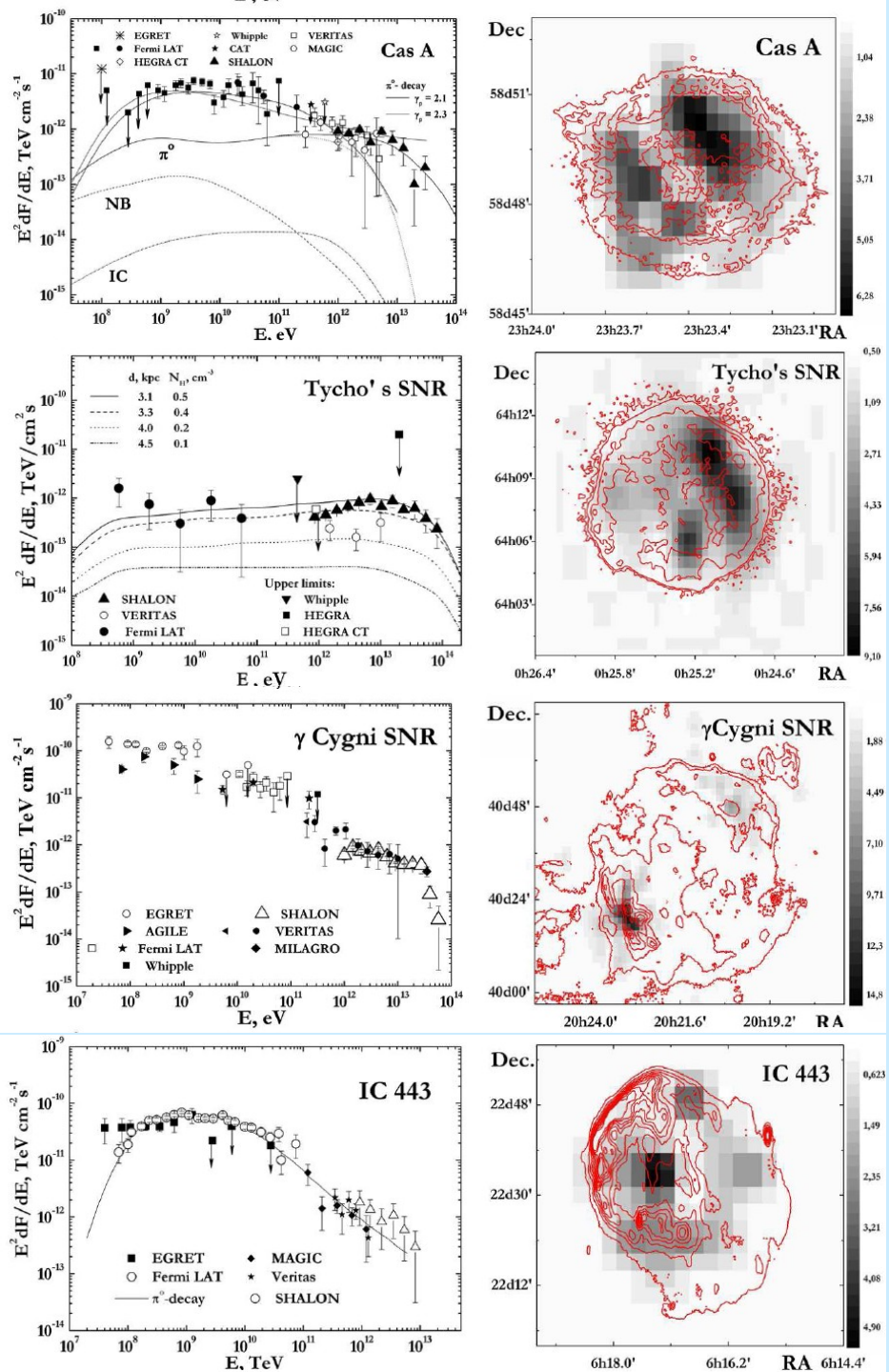

The observation results of Galactic shell-types supernova remnants on different evolution stages **GKPer (Nova 1901), Cas A (1680 yr), Tycho's SNR (1572yr), γCygni SNR age of (5÷7)×10³yr** and **IC443 age of (3÷30)×10³yr.** by SHALON mirror Cherenkov telescope are presented. The TeV γ-ray emission of **classical nova GK Per**, that could be a shell-type supernova remnant on early evolution stage, was detected for the first time by SHALON. Also, very high energy γ-rays from the **shell of GK Per**, visible in the X-rays, were detected with SHALON experiment for the first time. The experimental data have confirmed the prediction of the theory about the hadronic generation mechanism of very high energy γ-rays in Tycho's SNR, Cas A and IC443.

NGC 1275

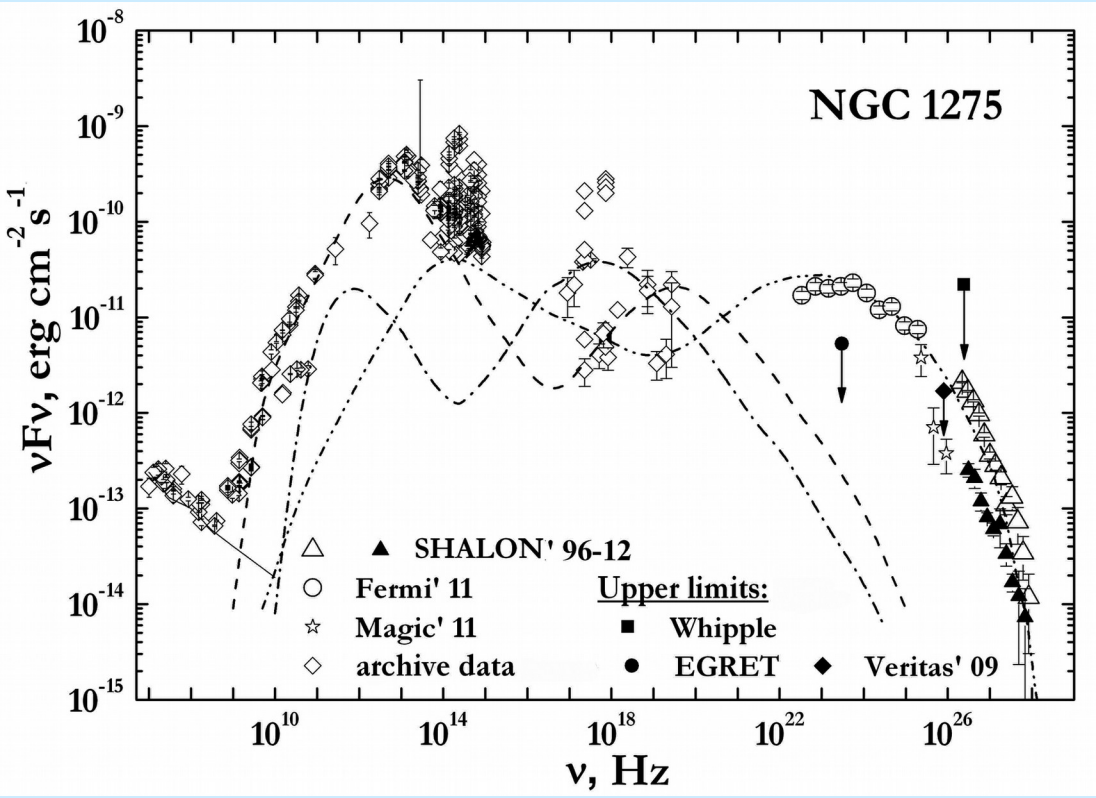

The multifrequency spectral energy distribution for the nucleus of NGC 1275, up to high and very high energies, was described in the CM model (Colafrancesco et al. 2010) and is a composition of the components of inverse Compton scattering of the intrinsic synchrotron radiation from relativistic electrons (synchrotron self-Compton) of three separate plasma blobs ejected from the inner regions of the NGC 1275 nucleus (the dashed, dash–dotted, and dash–dotted with two dots curves).

Overall spectral energy distribution of NGC 1275. The TeV energy spectrum of NGC 1275 from SHALON, 15 year observations in comparison with other experiments: Fermi LAT'09-11, MAGIC'10-11 and upper limits: EGRET'95 , Whipple'06, Veritas'09 and models.

The available Fermi LAT data at high energies and the SHALON observations at very high energies in a region < 32" around NGC1275 are described in terms of this model with one of the components produce synchrotron self-Compton emission of the relativistic jets from the nucleus itself (the dash–dotted with two dots curve).

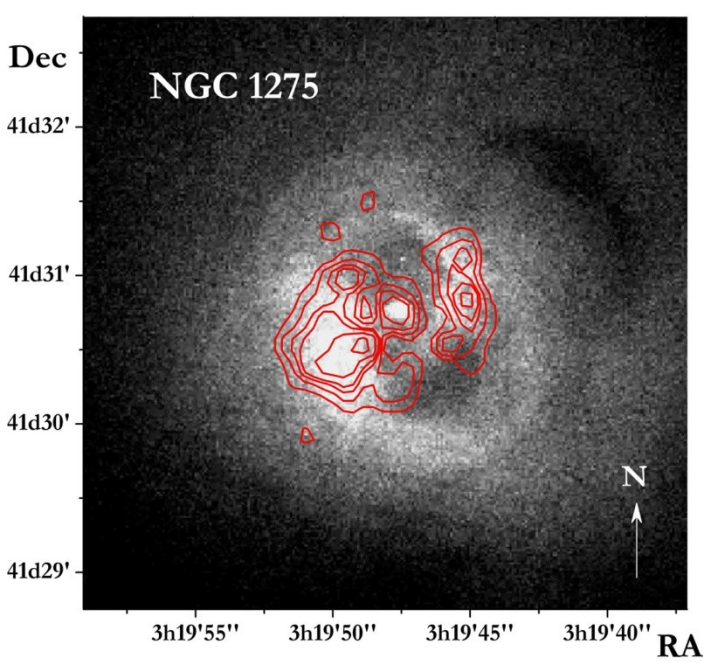

NGC 1275

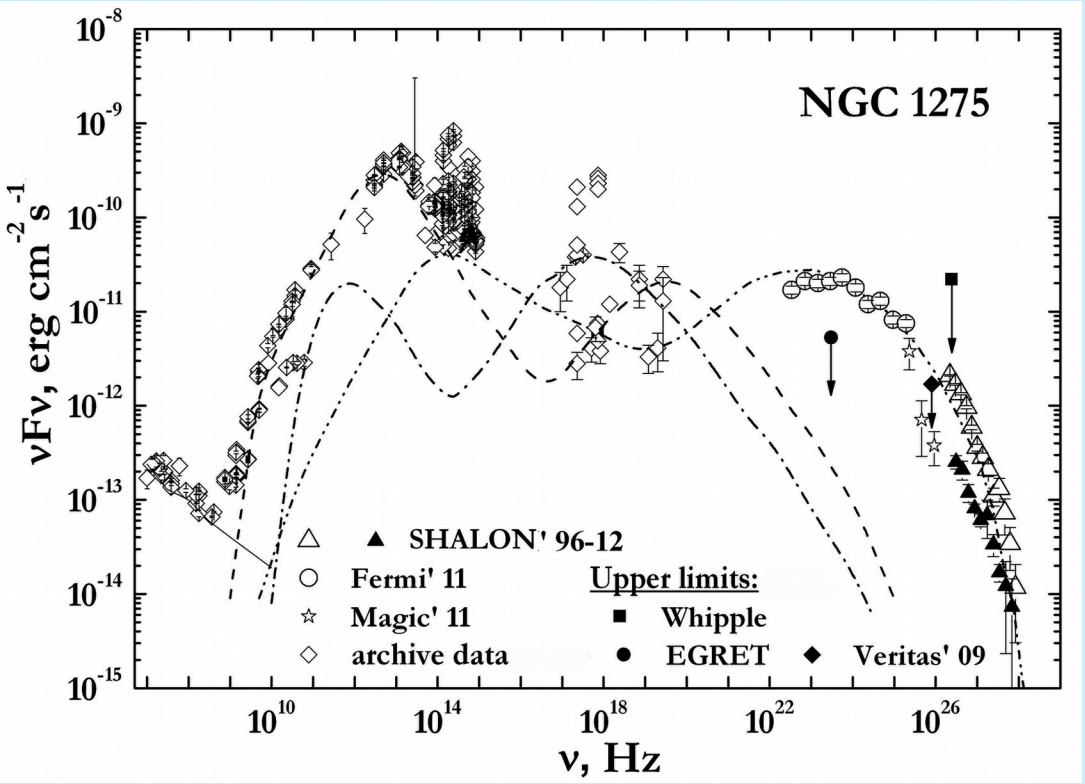

The TeV structure around NGC 1275 that spatially coincides with the X-ray emission regions can be produced by mechanisms related to the generation of an X-ray structure. The brightness distribution of the X-ray emission and the observed TeV emission shows a sharp increase in intensity outside the bubbles blown by the central black hole and visible in the radio band. This suggests that the X-ray-generating particles are swept up from the region of the radio lobes under the pressure of cosmic rays and magnetic fields generated in the jets at the center of NGC 1275. The structures visible in TeV γ-rays are formed through the interaction of very high energy cosmic rays with the gas inside the Perseus cluster and interstellar gas heating at the boundary of the bubbles blown by the central black hole in NGC 1275.

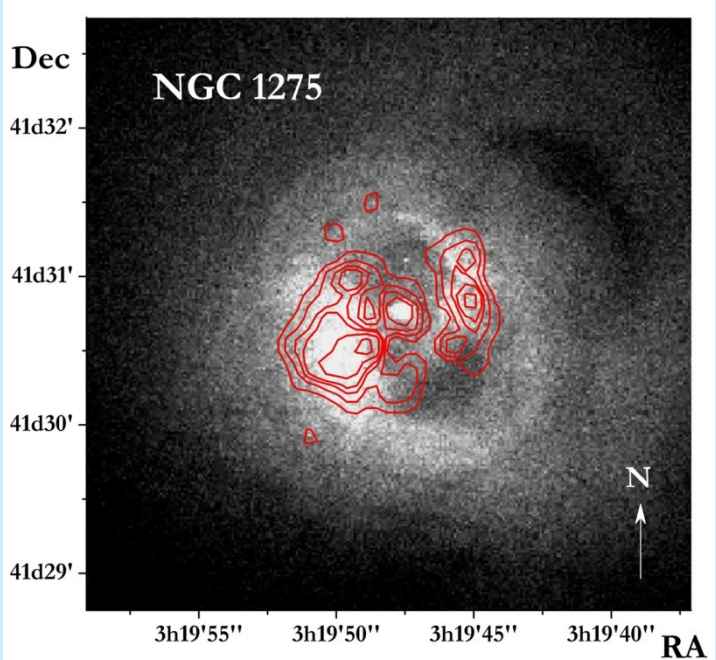

Overall spectral energy distribution of NGC 1275. The TeV energy spectrum of NGC 1275 from SHALON, 15 year observations in comparison with other experiments: Fermi LAT'09-11, MAGIC'10-11 and upper limits: EGRET'95 , Whipple'06, Veritas'09 and models.

The presence of emission in the energy range 1–40 TeV from a central region of ∼32" in size around the nucleus of NGC 1275 (black triangles) and the short-time flux variability point to the origin of the very high energy emission as a result of the generation of jets ejected by the central supermassive black hole of NGC 1275.

Conclusion

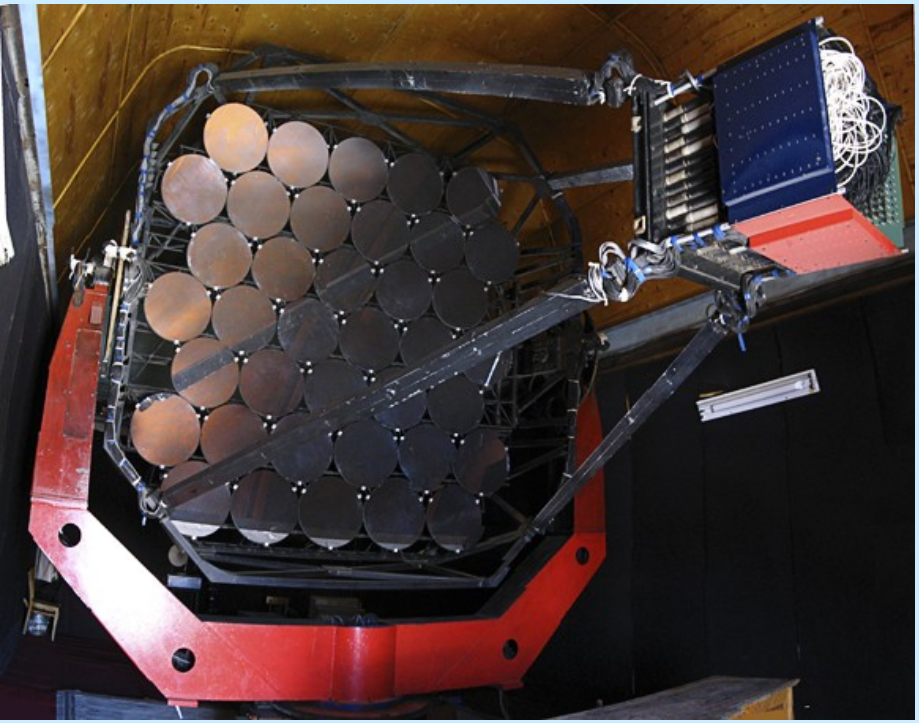

The cluster of galaxies in Perseus, along with other clusters, have long been considered as possible candidates for the sources of high and very high energy gamma-ray emission generated by various mechanisms. Long-term studies of the central galaxy in the cluster, NGC 1275, are being carried out in the SHALON experiment. We presented the results of fifteen-year-long observations of the AGN NGC 1275 at energies 800 GeV–40 TeV discovered by the SHALON telescope in 1996. The data obtained at very high energies, namely the images of the galaxy and its surroundings, and the flux variability indicate that the TeV gamma-ray emission is generated by a number of processes: in particular, part of this emission is generated by relativistic jets in the nucleus of NGC 1275 itself. Whereas, the presence of an extended structure around NGC 1275 is evidence of the interaction of cosmic rays and magnetic fields generated in the jets at the galactic centre with the gas of the Perseus cluster.

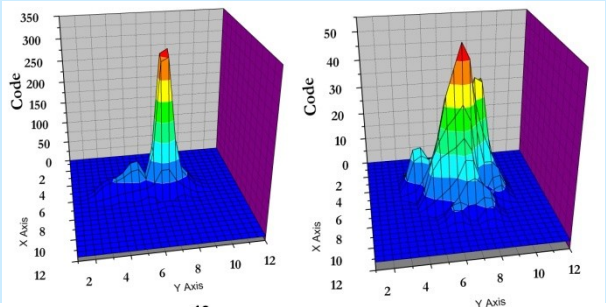

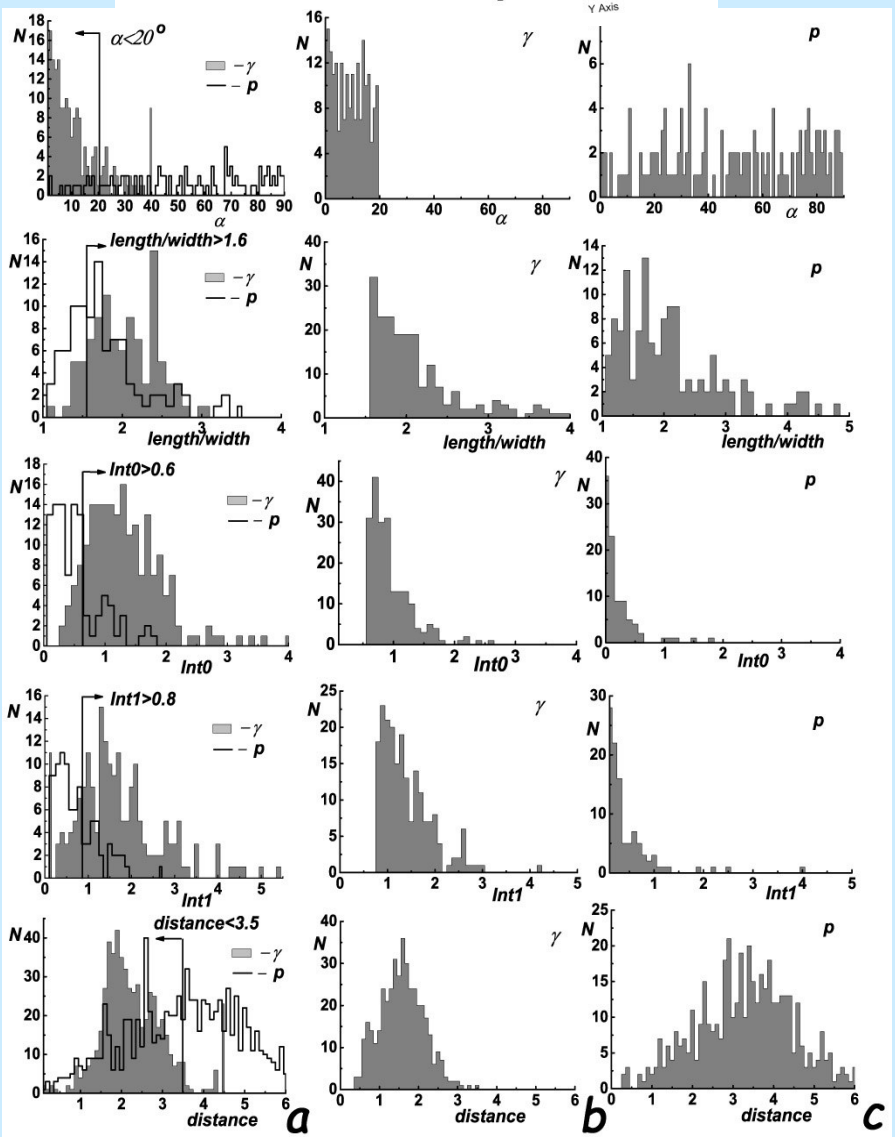

Criteria

The selection of gamma-initiated showers from the background of proton showers is performed by applying the following criteria:

1) **$\alpha < 20^o$; 72% rejection**
2) **length/width > 1.6**; **49% rejection**
3) the ratio **INT0** of Cherenkov light intensity in pixel with maximum pulse amplitude to the light intensity in the eight surrounding pixels exceeds > **0.6**; **92% rejection**
4) the ratio **INT1** of Cherenkov light intensity in pixel with maximum pulse amplitude to the light intensity in the in all the pixels except for the nine in the center of the matrix is exceeds > **0.8**; **88% rejection**
5) **distance** is less than **3.5** pixels. **50% rejection**

It is essential that our telescope has a large matrix with full angle >8° that allows us to perform observations of the supposed astronomical source (ON data) and background from extensive air showers (EAS) induced by cosmic ray (OFF data) simultaneously.

Using these criteria the background is rejected with 99.92% efficiency, whereas gamma's rejection is no more than 35% (that is taking into account) and the amount of background gamma-like events is less than 10%.

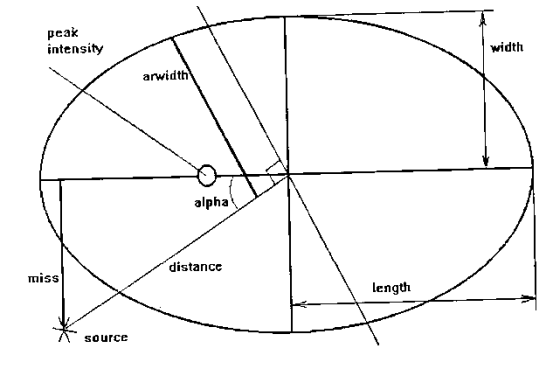

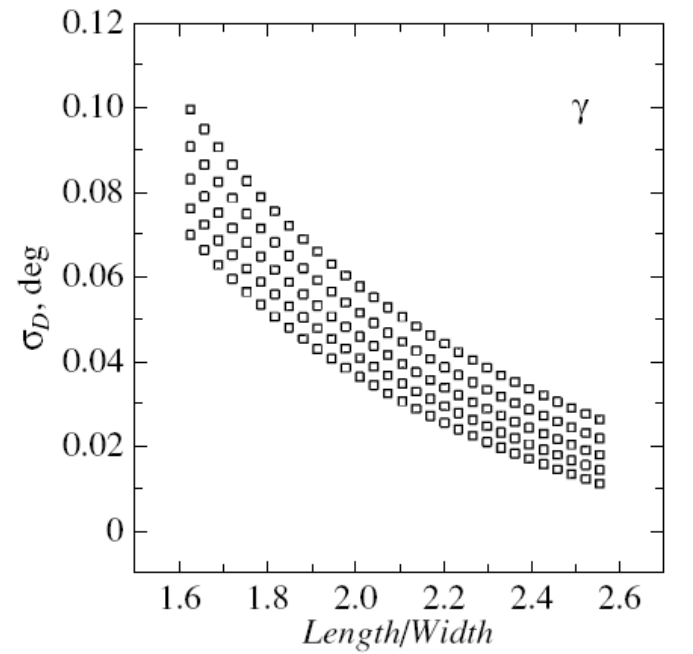

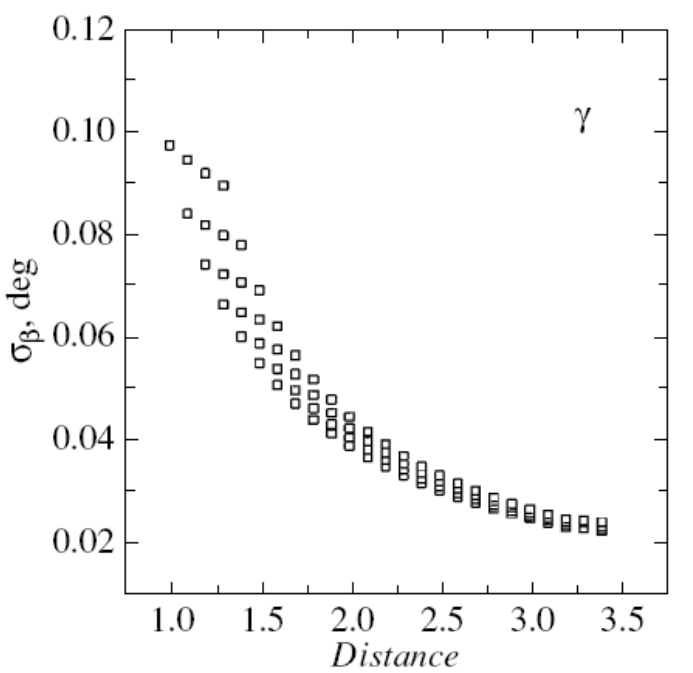

At the first step, the coordinates of the shower source position on the light receiver plane for each of the showers selected according to the described criteria are found. The shower image in the array is characterized by an ellipse with the major axis that is the projection of the shower axis onto the light receiver plane. The gamma-ray shower source is on the extension of the major axis of such an ellipse from the side of the shower maximum corresponding to the cascade beginning. The distance from the centroid of the shower image to the source's position, D, depends on the distance at which the shower arrived and, as a result, on the shower elongation by the parameter *Length*/*Width*. This dependence can bewritten as $D = B\times[1-(Length/Width)^{-1}]$. The optimal proportionality coefficient $B = 5.1$ was chosen in such a way that the distribution of shower arrival directions in angles was minimal in width and centered at the source's position on the array.

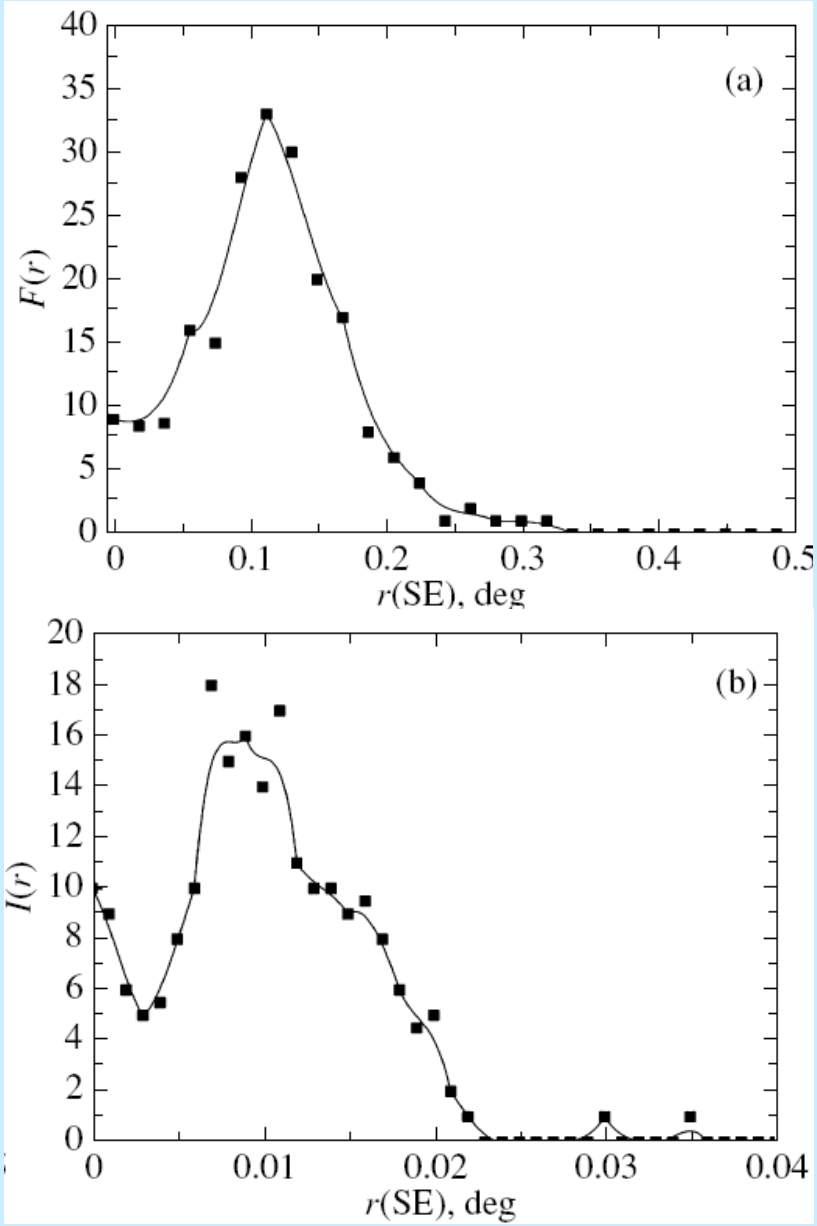

At the second step, an additional analysis of the gamma-ray shower source coordinates obtained at the first step is performed and the gamma-ray intensity distribution in the source is found. Finding the gamma-ray intensity distribution in the source $I(r)$ is reduced to solving a Fredholm integral equation of the first kind:

$$F(z) = \int K(r,s)I(s)ds$$

where $K(r, s)$ is the kernel function defined as a Gaussian point spread function with the full widths half magnitude σ_D and σ_β determined at the first step. Then, we refine the observed distribution from (a) by solving an integral equation under the assumption that the solution is a smooth nonnegative upper-bounded function, as the source's angular sizes were limited, and the solution was definitely within the region determined at the first step. Fig (b) presents the corrected gamma-ray intensity distribution *I(r)*, where r(SE) is the distance to the southeast from the nucleus of NGC 1275 in degrees. As a result of the second step, the accuracy of the determination of the coordinates of the gamma-ray shower source increases by a factor of ~10 compared to the first step and it becomes possible to find the gamma-ray intensity distribution in the source and its surroundings.

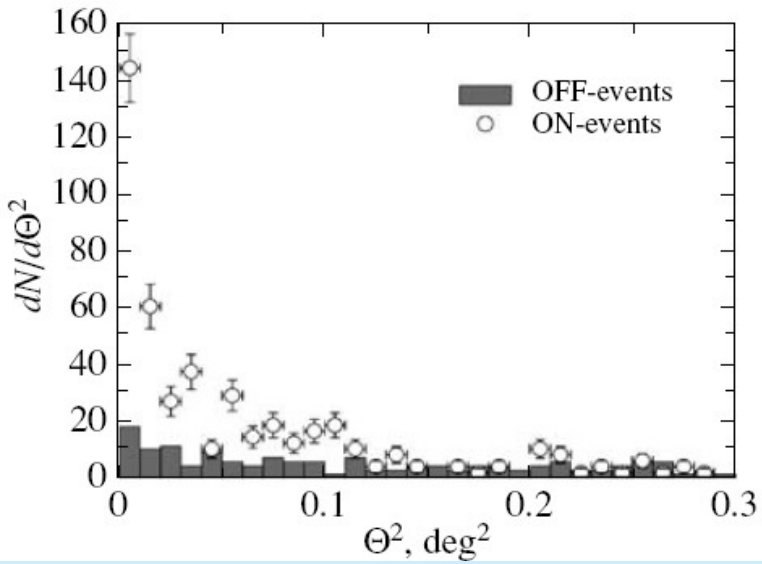

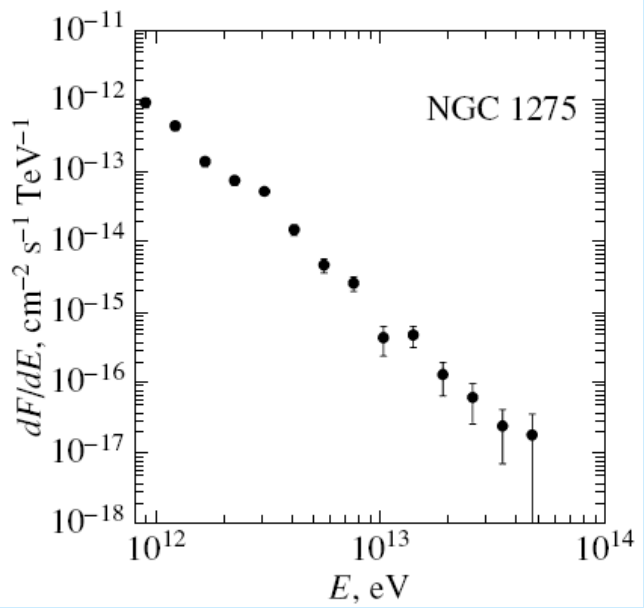

Differential spectrum of NGC 1275 from SHALON data.

Flux measurements in each energy interval

E, TeV	Excess	σ, Li and Ma	dF/dE, cm^{-2} s^{-1} TeV^{-1}
0.904	39	8.3	$(9.59 \pm 1.53) \times 10^{-13}$
1.22	54	10.6	$(4.45 \pm 0.60) \times 10^{-13}$
1.66	41	8.9	$(1.39 \pm 0.22) \times 10^{-13}$
2.25	47	9.8	$(7.52 \pm 1.01) \times 10^{-14}$
3.05	64	14.5	$(5.26 \pm 0.65) \times 10^{-14}$
4.13	34	10.3	$(1.51 \pm 0.26) \times 10^{-14}$
5.60	19	8.2	$(4.76 \pm 0.91) \times 10^{-15}$
7.59	18	8.1	$(2.63 \pm 0.62) \times 10^{-15}$
10.2	6	4.3	$(4.44 \pm 1.98) \times 10^{-16}$
13.9	10	5.9	$(4.83 \pm 1.61) \times 10^{-16}$
18.9	5	4.0	$(1.32 \pm 6.62) \times 10^{-16}$
25.6	4	3.8	$(6.27 \pm 3.62) \times 10^{-17}$
34.7	2	2.7	$(2.47 \pm 1.75) \times 10^{-17}$
47.0	1	1.5	$(1.75 \pm 1.00) \times 10^{-17}$

The distribution in Θ^2 for the signal (ON) and background (OFF) events recorded during the observations of NGC 1275 in the SHALON experiment in 271.2 h. Θ^2 is the distance between the source's position and the shower direction to the source reconstructed in the experiment. The observed excess corresponds to 31.4σ determined according to Li&Ma (1983).

The table gives the signal excess above the background for each energy interval of the differential spectrum, the signal detection confidence level according to Li and Ma (1983) in each interval, and the differential flux.